UNIVERSITY OF CINCINNATI

May 30 , 2003

I, Nanette Leann Dragula ,

hereby submit this as part of the requirements for the degree of:

Master of Science

in Pharmaceutical Sciences

It is entitled Localization of Glycosyl Phosphatidylinositol Anchored Acetylcholinesterase to Lipid Rafts of Caco-2 Cells

Approved by:

Kenneth A. Skau, Ph.D., Chair

Arthur R. Buckley, Ph.D.

Giovanni M. Pauletti, Ph.D.

LOCALIZATION OF GLYCOSYL PHOSPHATIDYLINOSITOL ANCHORED ACETYLCHOLINESTERASE TO LIPID RAFTS OF CACO-2 CELLS

A thesis submitted to the

Division of Research and Advanced Studies
of the University of Cincinnati

in partial fulfillment of the
requirements for the degree of

MASTER OF SCIENCE IN PHARMACEUTICAL SCIENCES

in the Division of Pharmaceutical Sciences
of the College of Pharmacy

2003

by

Nanette L. Dragula

B.S., Purdue University, 1999

Committee Chair: Kenneth A. Skau, Ph.D.

Localization of glycosyl phosphatidylinositol-anchored acetylcholinesterase to lipid rafts of Caco-2 cells

Lipid rafts are concentrated in the apical membrane of polarized cells where certain proteins, including those anchored by glycosylphosphatidylinositol (GPI) and several involved in signaling, are targeted. Acetylcholinesterase (AChE) is best known for its enzymatic activity at the neuromuscular junction and in synapses, where one of the three known splice variants, AChE-S (synaptic), hydrolyzes acetylcholine. AChE-E, or erythrocytic, is known to exist in human erythrocytes anchored by a GPI-moiety, and a readthrough form, AChE-R, has been found as a soluble monomer produced in response to stress. The existence of these various forms in many non-neuronal cells suggests that AChE may have some non-enzymatic functions, including a role in hematopoiesis, cell adhesion and tumorigenesis. In this study, AChE was investigated in cultured Caco-2 cells, a well-polarized, human, model intestinal epithelial cell line. Using phosphatidylinositol-specific phospholipase C, it was characterized as a GPI-anchored protein. Cells grown on transwell membranes exhibited AChE activity on the apical membrane that was six fold greater compared to the basolateral membrane. It was determined that AChE was three fold more soluble in octyl glucoside than in non-ionic detergents, such as Triton X-100. This observation supports its existence in lipid rafts. Another characteristic of lipid raft-associated proteins is the flotation in density gradients, such as the commercially available reagent known as Optiprep. AChE was found to float near fractions 14 and 15 in a 10-40 percent Optiprep gradient, where fraction 17 is the top. Results from immunofluorescent confocal microscopy indicated that AChE co-localized with ganglioside GM_1, which is a known lipid raft marker. Finally, reverse

transcription-polymerase chain reaction (RT-PCR) was performed to determine which specific AChE mRNA splice variants are expressed in Caco-2 cells. The readthrough transcript (AChE-R) was identified at low levels, whereas the synaptic and erythrocytic forms were found to be present in equal quantities, each more than two fold greater compared to AChE-R. These results indicate the presence of a GPI-anchored form of AChE associated with lipid rafts of Caco-2 cells. Message for the synaptic form is also present and may explain the AChE activity observed subsequent to Triton X-100 solubilization. The transcript for AChE-R is also expressed; however, we have found no evidence of a soluble form in Caco-2 cells. Possible functions for AChE in Caco-2 cells include cell proliferation or cell adhesion. AChE may also be a part of a complete cholinergic system in these epithelial cells that could act in the secretion of water and ions.

ACKNOWLEDGEMENTS

Many people deserve to be acknowledged for their help in making this thesis possible. I would first like to thank my advisor, Dr. Kenneth Skau, for his encouragement during my times of frustration and for his useful advice and guidance through this project. I would like to acknowledge my committee members, Dr. Arthur Buckley and Dr. Giovanni Pauletti, for their willingness to listen and offer suggestions. I would like to thank all of the University of Cincinnati School of Pharmacy faculty members and students for offering the use of their lab equipment as well as advice on techniques I was unfamiliar with. I would like to express my deepest gratitude for my parents. I thank my father for sharing his knowledge and words of wisdom through the years. I thank my mother for always expressing great pride and confidence in me, and I thank my stepfather for always recognizing my accomplishments and encouraging me to pursue my endeavors. My soon-to-be husband, Chris, has offered constant love, understanding, and compassion, even when it might have been difficult. I appreciate everyone who has contributed to my completion of this program. Thank you.

TABLE OF CONTENTS

LIST OF FIGURES

INTRODUCTION

Acetylcholinesterase

The cholinesterases have been studied for almost 90 years and is, therefore, one of the most well characterized groups of enzymes. Acetylcholinesterase (AChE, EC 3.1.1.7) and butyrylcholinesterase (BuChE, 3.1.1.8) can be distinguished by their specificity for different choline esters. Butyrylcholinesterase exhibits less substrate specificity and is able to hydrolyze acetylcholine (ACh), although it prefers butyrylcholine, as well as many other alkyl esters (Soreq and Zakut, 1993). The primary function of AChE is to rapidly hydrolyze ACh (Figure 1b) and inactivate cholinergic transmission at the neuromuscular junction and cholinergic synapses. However, AChE can be found in tissues that are not directly innervated by cholinergic nerves, and, despite the many years of studies, it is yet to be determined how it may alternately function in these tissues. One example is the presence of ACh-hydrolyzing activity in primitive organisms lacking a nervous system, such as *Paramecium* (Sastry and Sadavongvivad, 1979). It was proposed by Pantin (1956) that the cholinesterases may have been present prior to the development of the nervous system. Neuronal cells may have adapted the pre-existing cholinergic system to serve in neurotransmission. In addition, AChE can also be found in several non-neuronal cells of higher vertebrates including erythrocytes, neoplastic cells, and hematopoietic cells.

The active site of AChE consists of a catalytic triad made up of a serine, histidine, and an acidic residue, which varies among species (Figure 1a). X-ray crystallography of *Torpedo* AChE (Sussman et. al., 1991), and later human AChE (Kryger et. al., 2000),

revealed that this triad lies at the bottom of a 20-′ deep gorge lined with hydrophobic amino acid residues. In this gorge, there also exists a hydrophobic domain that is implicated in binding the charged choline ester. Additionally, there is a peripheral anionic site located more than 2 nm away from the active site. Ligand binding to this site has been proposed to cause allosteric changes in the protein (Soreq and Zakut, 1993). It is possible that toxic substances may bind here, and the conformational change might make AChE more efficient in scavenging these compounds. This site has also been implicated in some of the non-classical functions of AChE, which will be discussed below.

AChE exists in multiple isoforms differing in molecular weights, solubilities, and subunits. This diversity is produced by post-translational processing and alternative messenger RNA (mRNA) splicing of a single gene product. Massoulié et. al. (1999) reported two main isoforms that could be distinguished by their quaternary structure and anchoring mechanism (Figure 2). The globular form can exist as monomers, dimers, and tetramers. The asymmetric form consists of either a collagen-like tail or a hydrophobic tail tethered to the extracellular matrix and attached to catalytic tetramers (Massoulié et al., 1999). These forms are found most commonly at the neuromuscular junction and in the brain, respectively. The globular and asymmetric forms are then grouped by their C-terminal regions, which define distinct anchoring properties. Massoulié (1999) suggested the nomenclature for these various isoforms. Under this system, the first type of subunit is designated 'H', or hydrophobic, because the C-terminal peptide is characterized by hydrophobic sequences. This region also contains a signal for the addition of a glycosyl phosphatidylinositol (GPI) anchor. Another subunit is the 'T' or tailed subunit. This

Figure 1.a) Structural features of acetylcholinesterase. X-ray crystallography identified an active site of AChE consisting of a catalytic triad at the bottom of a 20- deep gorge. There is also a peripheral site implicated in some of the non-classical functions of AChE. The choline binding site is lined with hydrophobic residues. b) Acetylcholinesterase reaction. An acetyl-AChE intermediate is formed with the release of choline. Hydrolysis of the intermediate releases an acetate.

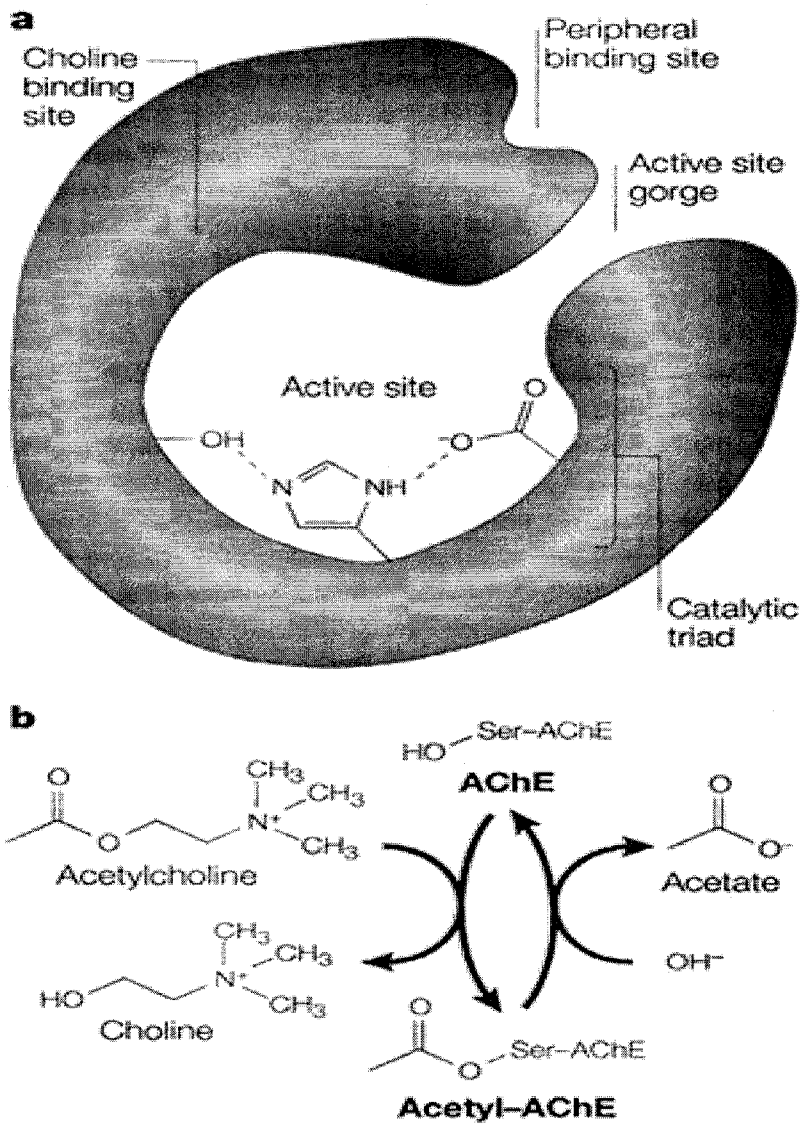

Soreq and Seidman, 2001

region is necessary for the assembly of collagen-tailed and hydrophobic-tailed molecules. The 'S' subunit (not shown) is so called because it has only been found in Elapid snakes as a secreted and soluble monomeric AChE in their venoms. Massoulié then defines a hypothetical readthrough ('R') transcript (not shown), which retains an intronic region following the last exon encoding the catalytic domain.

Soreq and Seidman (2001) described the three distinct mRNA species encoding AChE, each with a different carboxy-terminal sequence, which arise from alternative gene splicing (Figure 3). In this terminology, there is AChE-S (synaptic), which yields the E1-E2-E3-E4-E6 transcript. Translation results in an amphipathic multimeric protein that is found in brain and muscle tissues anchored to the membrane by either a hydrophobic subunit or a collagen tail. This is equivalent to Massoulié's 'T', or tailed subunit. The AChE-E (erythrocytic) transcript contains E1-E2-E3-E4-E5 and is similar to the hydrophobic form described above. This species yields a protein with a GPI group attached near the carboxyl terminus to anchor a dimerized subunit to the membrane and is found in human erythrocytes. The third variant, AChE-R (readthrough), is formed by continuous transcription through E1-E2-E3-E4-I4-E5. Translation results in a hydrophilic monomer that is expressed in cholinergic synapses where it is overproduced in response to stress (Meshorer et. al., 2002).

The diversity of the molecular forms and membrane-anchoring mechanisms suggests that AChE may have alternate functions other than the termination of cholinergic transmission. One of the proposed non-classical actions is the promotion of neuritogenesis (Soreq and Seidman, 2001). High levels of AChE can be detected in the embryonic nervous system well before the establishment of cholinergic transmission

Figure 2. Molecular forms of acetylcholinesterase. The globular (G) forms of AChE can exist as monomers, dimers, or tetramers. The asymmetric (A) form consists of a collagen-like tail attached to G4 subunits. The hydrophobic subunit contains a signal allowing the attachment of a GPI group and is found in human erythrocytes. The tailed forms contain either a hydrophobic tail or a collagen like tail and are found in brain and muscle tissue.

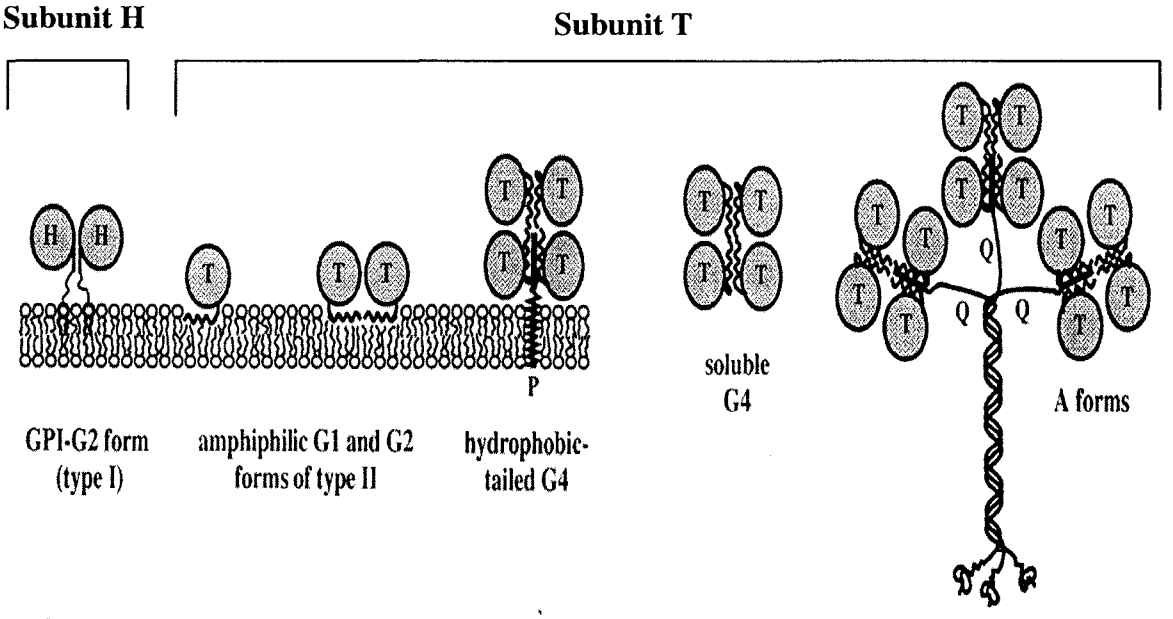

Massoulié et. al., 1999

Figure 3. Acetylcholinesterase splice variants. Three variants are described that differ in their carboxy terminal sequences. The synaptic (S) form splices out I4, E5, and E6 and is found in brain and muscle tissues. The erythrocytic (E) form contains E5, which allows for the attachment of a GPI anchor and is found in human erythrocytes. The readthrough (R) transcript contains the intron I4 followed by E5. It has been suggested that E5 is not transcribed so the protein exists as a soluble monomer in cholinergic synapses where it is produced in response to stress.

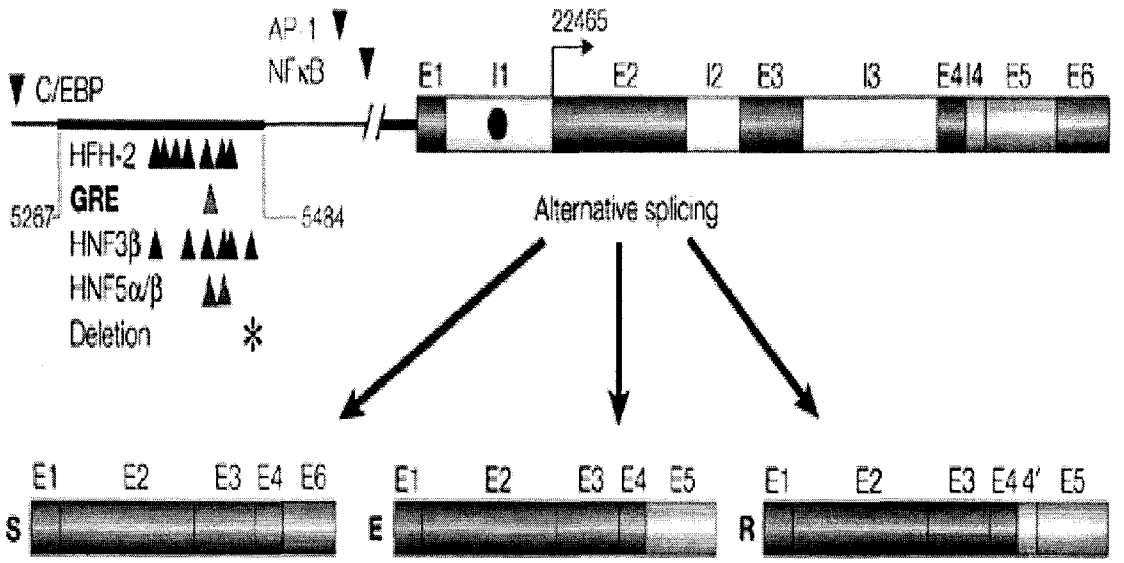

Soreq and Seidman, 2001

(Layer, 1983). It is also expressed in regions of the embryonic brain that do not show evidence later of cholinergic neurotransmission (Falugi and Raineri, 1985). Another indication that AChE may act in neuritogenesis is the observation that fasiculin-2, which binds selectively to the peripheral site of AChE, has been shown to inhibit neurite outgrowth, whereas inhibitors of the active site had no effect (Sharma and Bigbee, 1998).

Hematopoietic activities were first proposed based on the presence of AChE in blood-cell progenitors. AChE-R is overexpressed during stress in brain neurons, so a study was conducted to determine whether it may also play a role in the accelerated hematopoietic cell proliferation characteristic of a stress response. Human $CD34^+$ hematopoietic progenitor cells subjected to stress showed elevated AChE-R, and the cleavable C-terminal peptide of this variant, ARP, enhanced the proliferation of early hematopoietic progenitors (Deutsch et. al., 2002). Transcriptional activation of AChE was also observed during hemaglutinin-induced lymphocyte activation (Soreq and Seidman, 2001).

The high molecular and structural similarity AChE shares with the nervous system adhesive molecules neurotactin, neurolignin, and glutactin is an indication of its possible involvement in cell adhesion (Ilangurman et. al., 1999). This homology was localized to the N-terminal region of the extracellular domain, which would predict similar adhesive properties for all AChE variants and other roles for the distinct C-termini. In a study performed by Darboux et. al. (1996), the AChE-homologous region of neurotactin was replaced with the homologous *Drosophila* AChE core, and the chimera retained its adhesive properties.

Supporting a role in tumorigenesis, Perry et. al. (2002) correlated tumor

aggressiveness of astrocytomas with increased expression of AChE-R compared to AChE-S. It was also observed that the over-expression of AChE-R in glioblastoma cells was associated with a significant increase in cell proliferation. In addition, Karpel et. al. (1994) identified mRNA for a GPI-linked dimer readthrough in several tumor cells, including lung, kidney, and blood cells. Furthermore, Valero and Vidal (1995) found a GPI-linked monomer in human meningioma. These are all possible non-classical functions of AChE, which will need to be investigated further before any conclusions can be made.

Not only has AChE been found in non-neuronal cells, but also other molecules involved in cholinergic signaling have been found outside of the nervous system. These have been referred to as 'non-neuronal cholinergic systems' because they appear to be fully functional and involved in the regulation of important cell processes. Human bronchial epithelial and endothelial cells were reported to express nicotinic receptors, as well as the ACh synthesizing enzyme known as choline acetyltransferase (ChAT) and AChE (Wang et. al., 2001). A complete cholinergic system was also identified in human keratinocytes (Grando et. al., 1997), and it seems that the entire epidermal surface expresses ACh (Wessler et. al., 1998). Studies with epidermal keratinocytes have suggested that activation of the muscarinic ACh receptor affects cell attachment, spreading, and lateral migration (Grando et. al., 1997). Nicotine, an agonist of nicotinic receptors, also promoted wound healing implicating an involvement in epidermal cell proliferation. The same group of investigators identified a cholinergic system in human gingival keratinocytes that seems to be involved in cell cycle progression (Arredondo et. al., 2003). In a study with small cell lung carcinoma cell lines, nicotine was shown to

stimulate cell proliferation (Cattaneo et. al., 1997). In addition, there is evidence that non-neuronal cholinergic systems are involved in the secretion of ions, water, and macromolecules and in the regulation of ciliary activity (Wanner et. al., 1996). These systems may also contribute to immune functions and inflammatory actions.

In relation to the possible inflammatory function of a non-neuronal cholinergic system, it is known that ulcerative colitis occurs less frequently in smokers. Therefore, nicotine is thought to have a protective effect against this disease. Ulcerative colitis is a disease characterized by inflammation in the lining of the large intestine, most often in the lower colon. This is relevant to the work presented here because we have found AChE in a cell line derived from the epithelia of the colon. To date, there have been no reports indicating the existence of a non-neuronal cholinergic system in intestinal epithelia. The possible anti-inflammatory action of nicotine in the colon, though, indicates the presence of nicotinic receptors and the potential for cholinergic signaling.

Lipid Rafts

Most biological phospholipids have low melting temperatures (T_m), below which model membranes exist in a gel or frozen phase. The acyl chains of these frozen-state lipids are packed tightly together and have low rates of mobility and diffusion within the bilayer. Above the T_m of the phospholipid species, the bilayer is present in a liquid-crystalline, liquid-disordered (l_d) phase (Brown, 2002). This phase contains a high concentration of unsaturated, kinked fatty acid chains with high rates of mobility. Cellular membranes are generally thought to exist in this liquid-crystalline phase.

However, the plasma membrane of eukaryotic cells is also rich in sphingolipids, which have saturated acyl chains and a much higher T_m, and cholesterol. In a mixture of phospholipids and sphingolipids, high temperatures would favor the liquid-disordered phase, whereas, low temperatures would favor the gel phase. Cholesterol, though, increases the melting temperature of the bilayer, and complicates the phase behavior. In this case, at a temperature above the T_m of the phospholipid, a liquid-ordered (l_o) phase can separate from the liquid-disordered phase. This liquid-ordered phase has characteristics in between those of the gel phase and those of the liquid-disordered phase. As in the gel phase, the acyl chains of the lipids are ordered and tightly packed, but they have a high lateral mobility like in the liquid-disordered phase. Cellular sphingolipids have been reported to be insoluble in non-ionic detergents (Hagman and Fishman, 1982); so, the patches that sphingolipids and cholesterol form would remain after solubilization of the surrounding bilayer. Supporting this idea, plasma membranes have been found to be partially resistant to solubilization by Triton X-100 and most other non-ionic detergents at 4^0C (Brown and London, 1998). One exception is octyl-glucoside, which is structurally similar to a glycolipid and may be able to associate with the lipid patches allowing solubilization. There are two known types of detergent-resistant membranes; those that contain caveolin and those that do not. The microdomains that are enriched in caveolin form flask-shaped invaginations called caveolae, whereas, the non-caveolin domains have been termed 'lipid rafts' (Simons and Toomre, 2000).

An enrichment of glycosphingolipids in the apical versus basolateral membrane of the intestinal epithelial cell lines HT-29 and Caco-2 has been demonstrated (van't Hof and van Meer, 1990), indicating that the apical membrane likely contains these liquid-

Figure 4. Proposed lipid raft structure. Lipid rafts consist of saturated acyl chains including sphingolipids and GPI-anchored proteins on the external leaflet. Cholesterol molecules act as spacers in between the acyl chains. Src tyrosine kinases associate with rafts on the internal leaflet.

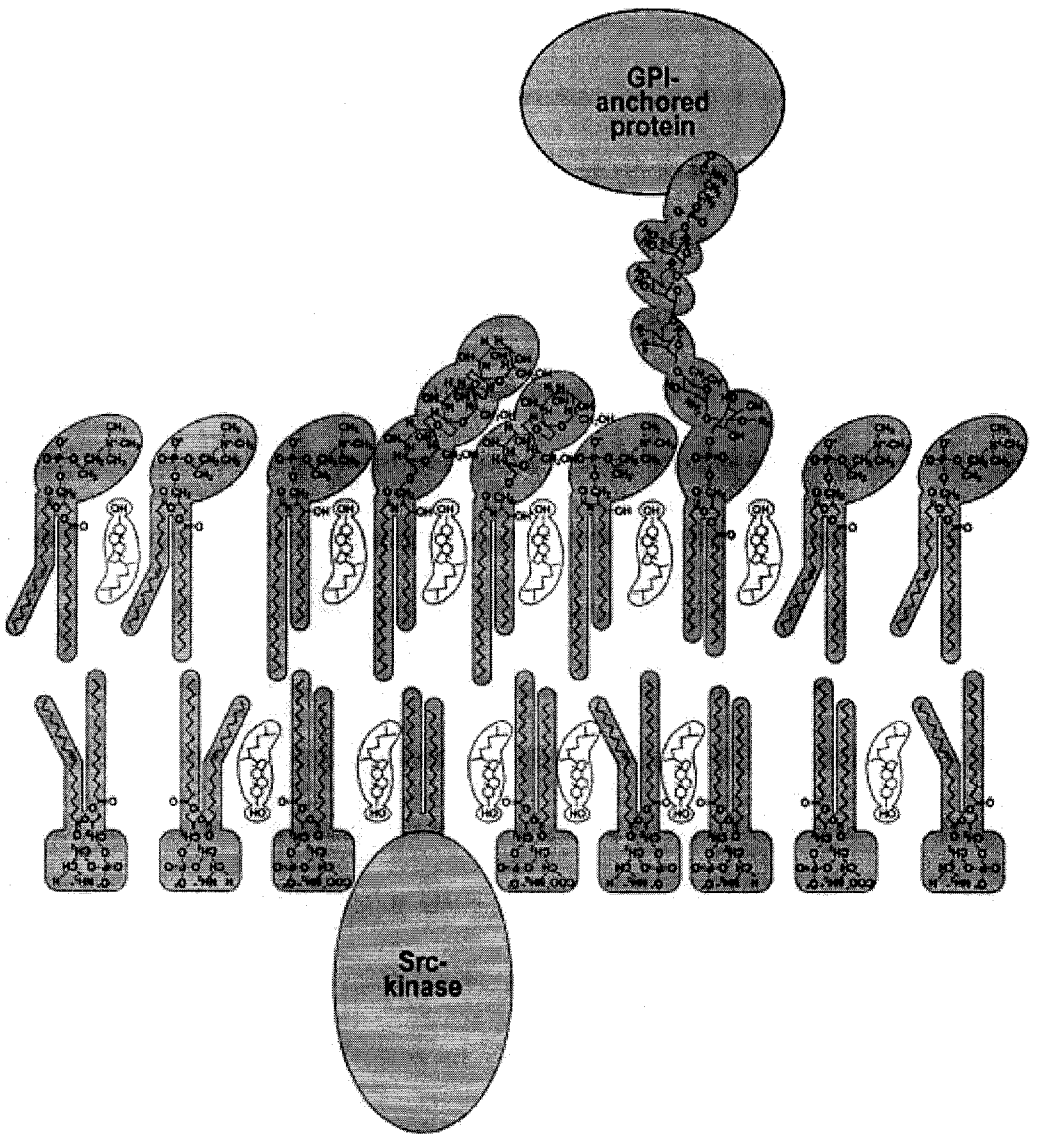

Simons and Ikonen, 1997

ordered microdomains. It was subsequently determined that Caco-2 cells do not contain caveolin, the protein required to form the domains called caveolae; so, they are designated as lipid rafts (Mirre et. al., 1996). Lipid rafts are proposed to contain tightly packed sphingolipids with cholesterol serving as spacers (Figure 4). They tend to float to a low density during density gradient centrifugation due to their high lipid content (Simons and Toomre, 2000). Proteins linked to dual saturated acyl chains, such as the tyrosine kinases of the Src family, and those anchored to the membrane by glycosyl phosphatidylinositol (GPI) are known to associate with these rafts. In addition, some transmembrane proteins are also found in lipid rafts, including the epidermal growth factor receptor (EGFR) and the T-cell receptor (TCR) (Zajchowski and Robbins, 2002).

It has been shown that the integrity of the rafts can be disrupted by extraction of cholesterol (Schroeder et. al., 1998). Once cholesterol has been extracted by such treatments as methyl β cyclodextrin (MβCD) or saponin, GPI-anchored proteins can be solubilized by Triton X-100 at 4^0C. However, other studies have demonstrated the existence of stable, cholesterol-independent microdomains. Although Hansen et. al. (2001) extracted 70% of the cholesterol from enterocyte brush border microvillar vesicles, they continued to find their raft marker protein in the floating fractions of the gradient. They attributed this to the high content of sphingolipids found in the brush border. Their hypothesis is supported by a study on model membranes where a high concentration of sphingolipids was shown to allow ordered phase formation in the absence of cholesterol (Schroeder et. al. 1998). In the model membranes containing high amounts of sphingolipids, Schroeder's group also determined that human placental alkaline phosphatase, a known GPI-anchored protein, was not Triton X-100 soluble after

saponin treatment. Another study on renal epithelial membrane models reported that cholesterol depletion does not suppress phase separation (Milhiet et. al. 2001). In these sphingolipid-enriched domains, they actually found a threshold close to the physiological concentration above which cholesterol acts as a suppressor of lipid rafts. It was also pointed out that a glycerophospholipid/sphingolipid/cholesterol ratio similar to that of renal epithelial cells exists in the apical membrane of intestinal epithelial cells. This is an indication that lipid rafts of the intestinal brush border membrane would be cholesterol independent as well. The addition of exogenous gangliosides, such as GM_1, has also been shown to cause a disruption of microdomains possibly by displacing the GPI-anchored proteins (Simons et. al., 1999).

Lipid rafts can include or exclude proteins; therefore, it seems logical that they may modulate and integrate signaling events by compartmentalizing the components involved. It has also been proposed that signaling molecules might be translocated into a lipid raft in response to stimuli (Figure 5) [Zajchowski and Robbins, 2002]. Supporting a role in signal transduction, specific G proteins (G_i and G_s), tyrosine kinases, and cross-linked T-cell receptors aggregate in lipid rafts (Simons and Toomre, 2000; Kovarova et. al., 2001). Studies of immunoglobulin E (IgE) signaling during the immune response have shown convincing evidence of the involvement of lipid rafts (Sheets et. al., 1999). IgE binds to receptors (FcεRI) in the plasma membrane of mast cells and basophils. Oligomeric antigen then binds IgE causing the crosslinking FcεRI and initiating the signaling cascade ultimately leading to the release of the chemical mediators of allergic reaction. It was found that after crosslinking, FcεRI becomes Triton X-100 insoluble. A redistribution of raft components, such as GPI-anchored proteins and gangliosides, to

patches visible by fluorescence microscopy is also observed (Stauffer and Meyer, 1997). More evidence comes from the finding that IgE signaling is abolished after depletion of cholesterol with methyl β cyclodextrin. These observations indicate that raft clustering occurs after receptor activation.

Signaling by GPI-anchored proteins has also been shown (Zajchowski and Robbins, 2002). It is unknown how the signal is transduced to intracellular effectors because these proteins have no transmembrane or cytoplasmic domains. It is believed that an interaction of the GPI-anchored protein with a transmembrane adaptor may occur, which would in turn signal an Src kinase on the internal leaflet. An example of this type of signaling involves the GPI-anchored protein, GDNF family receptor alpha (GFRα) [Zajchowski and Robbins, 2002).Glial cell line-derived neurotrophic factor (GDNF) binding results in the recruitment of the transmembrane receptor tyrosine kinase, Ret, to lipid rafts and the association with Src leading to downstream signaling. Figure 5 shows this proposed model of GPI-anchored protein signaling.

In addition to signal transduction, it has been proposed that these detergent-resistant membranes may act as a protein-sorting device in polarized cells (Brown, 1998). Because GPI-anchored proteins are found apically in epithelial cells and because sphingolipids are more concentrated in the apical membrane, it has been suggested that association with lipid rafts may be a sorting signal. Evidence comes from a study using polarized epithelial cells called Madin-Darby Canine Kidney cells (MDCK). The investigators inhibited sphingolipid synthesis and found that a GPI-anchored protein normally found apically was mis-sorted (Mays et. al., 1995). Alfalah et. al. (2002) studied the sorting behavior of the lipid raft associated protein, intestinal

Figure 5. a) Proposed model of lipid raft signaling by GPI-anchored proteins via transmembrane adaptors and Src family kinases. b) Model of signaling by a cell surface receptor translocated to lipid rafts upon ligand binding.

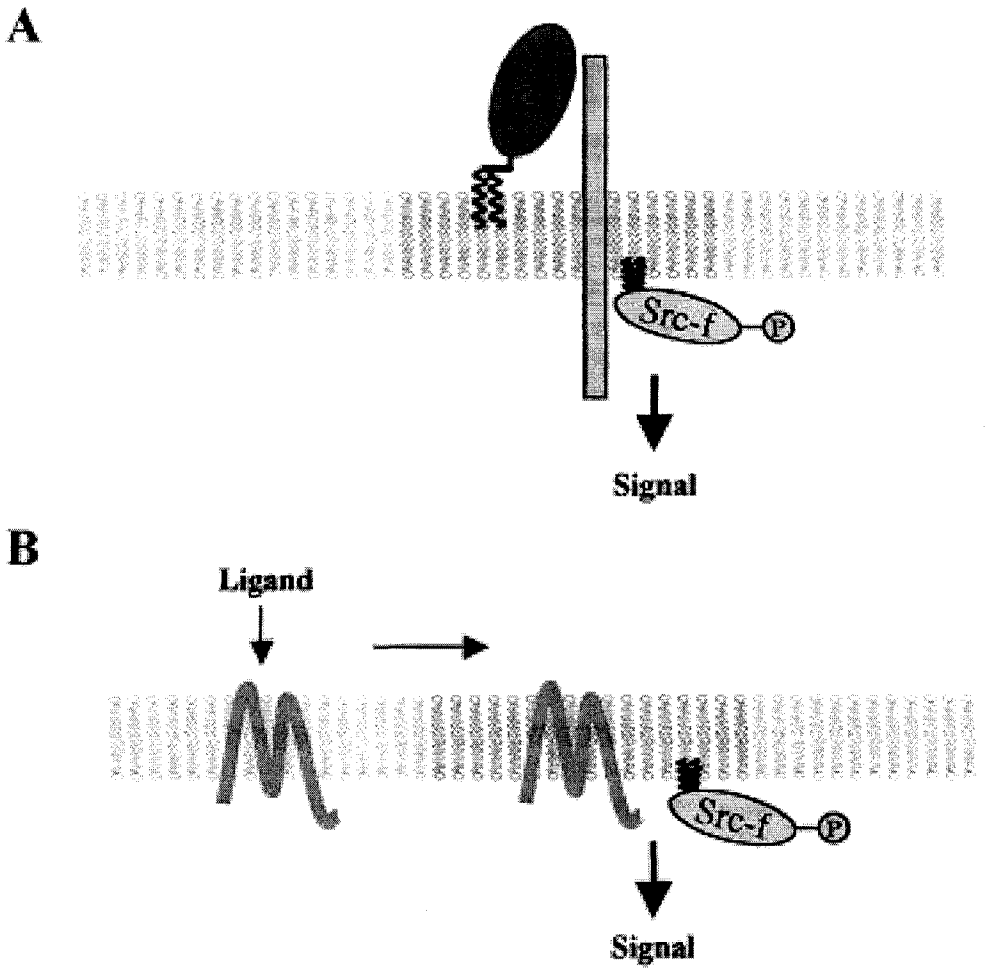

Zajchowski and Robbins, 2002

dipeptidyl peptidase IV (DPPIV), in Caco-2 and HT-29 cells. After cholesterol depletion with MβCD, 20% more DPPIV was found at the basolateral membrane than was found in the controls.

It has recently been suggested that lipid rafts play a direct role in the assembly of adhesion complexes. Many cell adhesion molecules are anchored to the membrane by a GPI moiety and are therefore, recruited into lipid rafts. Stable cell-cell adhesion requires strong binding forces, and to fulfill this requirement, single adhesion molecules must oligomerize into lattices. The clustering of GPI-anchored adhesion molecules in lipid rafts promotes this oligomerization. This interaction has been shown in studies on the *Dictyostelium* adhesion molecule gp80, which mediates cell-cell adhesion via homophilic interactions during the early stages of *Dictyostelium* development and can be found in Triton X-100 insoluble, floating fractions (Harris et. al., 2001). During the formation of cell-cell contacts, *Dictyostelium* cells were exposed to an anti-gp80 antibody followed by secondary antibodies. The cells were then subjected to filipin staining to detect sterol-rich domains. Microscopy revealed the co-localization of gp80 and sterols in initial patches that grew with time to form large micrometer-size domains at cell-cell contacts.

Glycosyl phosphatidylinositol-Anchored Proteins

Glycosyl phosphatidylinositol-anchored proteins (GPI-AP) consist of a single phospholipid spanning the exoplasmic leaflet of the membrane linked to an inositol, a glucosamine, a chain of three mannose sugars, and a phosphoethanolamine to which is attached the protein via an amide bond (Chatterjee and Mayor, 2001) [Figure 6a]. The

GPI anchor is synthesized on the cytoplasmic side of the rough endoplasmic reticulum (ER) and is then flipped across the membrane before addition of the protein. In mammalian GPI anchor precursors, the inositol is additionally acylated early on, which renders the structure resistant to cleavage by phosphatidylinositol-specific phospholipase C (PI-PLC) [Hooper, 1997]. This additional acyl group is removed in most GPI-anchored proteins before it arrives at the cell surface. A rare exception is human erythrocytic AChE, where it is present in the mature protein (Figure 6b) rendering it resistant to phosphatidylinositol-specific phospholipase C (PI-PLC). The nascent protein initially contains a hydrophobic N-terminal sequence that directs it into the lumen of the rough endoplasmic reticulum (ER) where the sequence is cleaved (Hooper, 1997). The pre-formed GPI-anchor is then attached to the new carboxyl terminus transamidase. This process results in the localization of the protein to the exoplasmic leaflet of the membrane, and specifically to the apical side of polarized cells.

The primary function of a GPI anchor is membrane attachment, as is the function of a single membrane-spanning polypeptide anchor. However, GPI anchors have characteristics not shared by polypeptide anchors that allow for additional functions. Cleavage by a phospholipase C or D would allow for a down-regulation of the protein from the cell surface and the release of a soluble form that could act at distant sites (Hooper, 1997). This type of anchor consumes less space in the membrane than a transmembrane protein and enables dense packing. They are also more laterally fluid since they do not interact with intracellular cytoskeletal proteins. Most GPI-anchored proteins are insoluble in Triton X-100 and other non-ionic detergents, which is surprising because the hydrophobic phosphatidylinositol group would be expected to partition into

Figure 6. a) Structure of a glycosyl phosphatidylinositol-anchor from porcine kidney membrane dipeptidase and the relative distribution and structures of the side-chain modifications (X and Y). Arrow identifies site of cleavage by PI-PLC. b) Comparison of representative glycosyl phosphatidylinositol-anchored proteins. Erythrocytic AChE (E) contains an additional acyl group that renders it resistant to cleavage by PI-PLC.

A

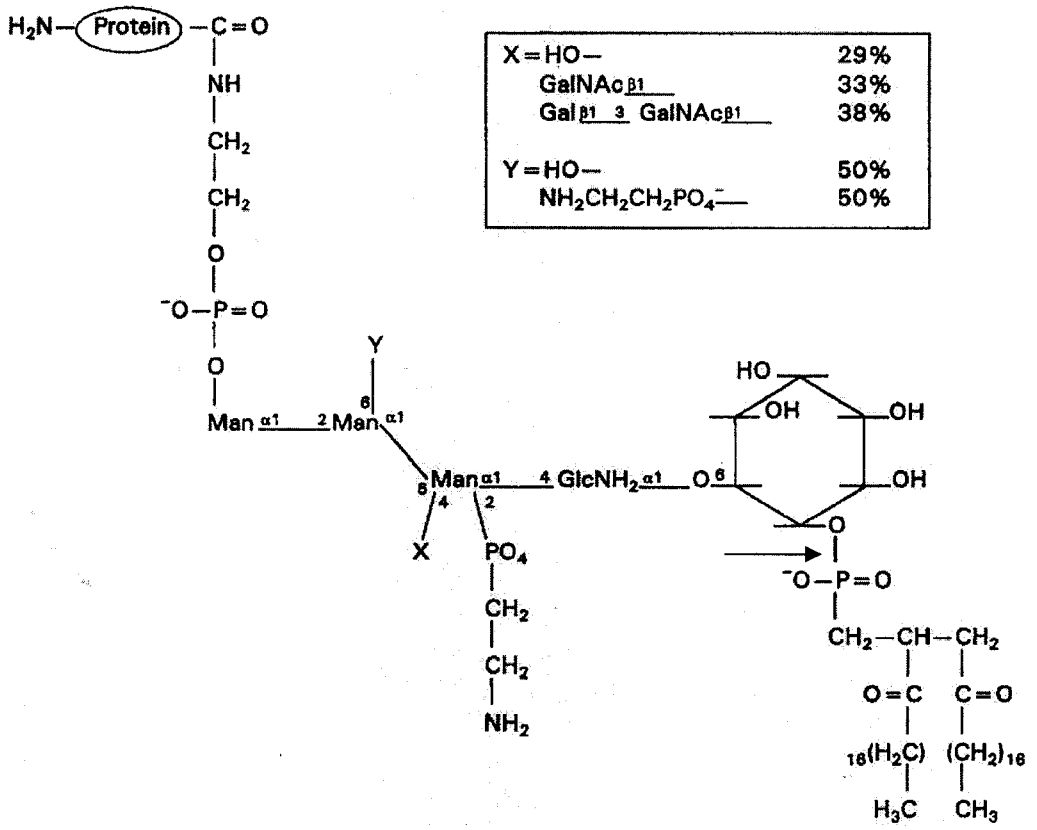

Hooper, N., 1997

B

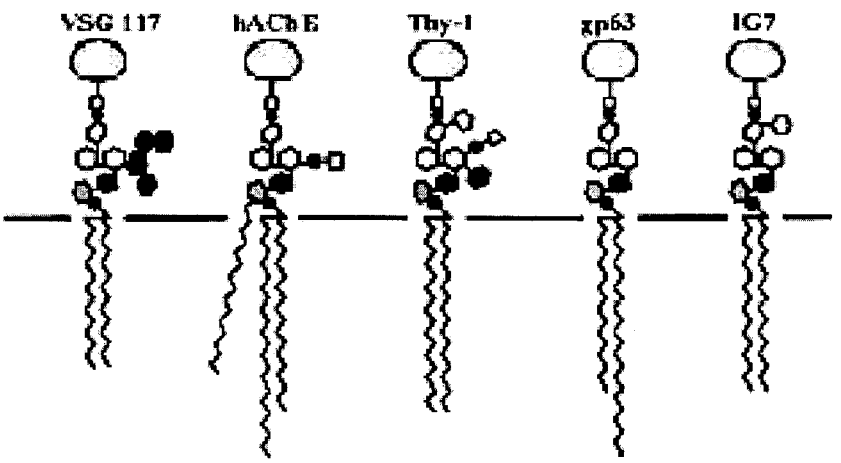

Chatterjee and Mayor, 2001

detergent micelles. In a particular GPI-anchored protein, placental alkaline phosphatase, the insolubility was acquired once it reached the Golgi apparatus (Brown and Rose, 1992). It is believed to occur by the preferential association of lipids in the GPI-anchor with sphingolipids destined for the membrane where they will form lipid rafts. The observation that sphingolipids are synthesized in post-ER compartments is consistent with this model. One GPI-anchored protein that has not yet been demonstrated as residing in detergent-resistant membranes is AChE. The erythrocytic form is soluble in Triton X-100 and is not characterized as a lipid raft protein.

GPI-anchors can be found on many diverse molecules. These include enzymes such as alkaline phosphatase, adhesion molecules such as NCAM, and receptors such as the folate receptor (Chatterjee and Mayor, 2001). Therefore, these GPI-anchored proteins have therefore been implicated in signaling cascades and in cell adhesion. As discussed above, the anchor has also been proposed to be an apical targeting signal during sorting and transport. Some of the apically targeted GPI-anchored proteins contain an apical sorting signal in their ectodomain (Brown and Rose, 1992). Those that do not, though, are still somehow delivered to the apical membrane. The crosslinking of GPI-anchored proteins has been shown to result in many intracellular responses including Ca^{2+} influx, cytokine secretion, and proliferation (Ilangumaran et. al., 1999). Alternatively, the GPI-anchored proteins may interact laterally with transmembrane proteins, which in turn may signal an Src family kinase attached to the cytoplasmic leaflet of the membrane.

Many cell adhesion molecules are anchored by a GPI moiety. Two such known molecules, NCAM and contactin, are both important in neurite outgrowth. As demonstrated with gp80 in *Dictyostelium*, the recruitment to lipid rafts might promote the

formation of large adhesion complexes necessary for the stable cell-cell interactions required for neuronal development (Harris, 2001). There are also GPI-anchored adhesion molecules outside of the nervous system. One immunologically important protein is the lymphocyte function-associated antigen 3 (LFA-3) (Dustin et. al., 1987). LFA-3 participates in adhesion between T-cells and the antigen-presenting cell aiding in the recognition and processing of antigen. The presence of the GPI-anchor on LFA-3 may have a significant advantage over the polypeptide-anchored form due to the increased lateral mobility, which would allow quick diffusion to the sites of adhesion.

Caco-2 Cells

We have characterized AChE found in enterocytes using the Caco-2 cell line. This human colon adenocarcinoma cell line is well-established as an *in vitro* model for studying some properties of intestinal epithelia. These cells spontaneously differentiate in culture forming a polarized monolayer with the apical side facing the medium. Studies have shown that Caco-2 cells exhibit structural and functional differentiation patterns characteristic of mature enterocytes (Pinto et. al., 1983). Electron microscopy has revealed the development of brush border microvilli on the apical surface, and they show high levels of the brush border enzymes alkaline phosphatase, sucrase-isomaltase, and some aminopeptidase (Pinto et. al., 1983). The functional differentiation of the cells is associated with the formation of domes by the microvilli, which is typical of transporting epithelial monolayers. Therefore, Caco-2 cells are commonly used in drug transport studies. They were used in the present studies as a model of carcinomic, intestinal

epithelial cells. As of yet, there have been no published results characterizing AChE as a lipid raft protein in Caco-2 cells.

Summary

In addition to inactivating acetylcholine (ACh) in synapses and at the neuromuscular junction, acetylcholinesterase (AChE) has been implicated in several non-catalytic functions. The diverse range of molecular isoforms and membrane-anchoring mechanisms of AChE has led to this proposal. These different types of anchors can act as localization signals, directing the molecule to specific areas of the cell (Massoulié et al., 1999). Another indication that AChE may have alternate functions is the observation that it is found in many tissues that are not directly innervated by cholinergic nerves and in embryonic tissues before the development of the nervous system (Layer, 1983).

AChE exhibits a high molecular and structural homology with some adhesion molecules, including neuroligin, glutactin, and neurotactin which may indicate a potential role for the protein in cell adhesion. Evidence for an involvement in neuritogenesis has been shown by the inhibition of neurite outgrowth by fasiculin-2 (Sharma and Bigbee, 1998), which binds specifically to the peripheral site of AChE. Evidence has also been presented implicating a function in hematopoiesis. It has been proposed that AChE is involved in tumorigenesis. In humans, the GPI-linked variant is only known to exist in erythrocytes, but it has now been found in many tumor cell types (Valero and Vidal, 1995). The readthrough form of AChE is produced in the brain in response to stress, but

some investigators have also observed it in tumor cells anchored to the membrane by a GPI-anchor (Karpel et. al., 1994).

Lipid rafts have been identified in a wide range of cell types. They are characterized by tightly packed sphingolipids with cholesterol serving as spacers. Proteins linked to saturated acyl chains are enriched in lipid rafts, including GPI-anchored proteins and doubly acylated tyrosine kinases. Since lipid rafts can preferentially include or exclude proteins, they have been implicated in some important cellular functions. Several signaling molecules have been localized to lipid rafts, including some G proteins, Src-family kinases, Ras, PKCa, and adenylate cyclase; therefore, lipid rafts may facilitate signaling events (Simons and Toomre, 2000). Lipid rafts are found apically in polarized epithelial cells and may act to sort proteins during transport (Brown, 1998). Recently, lipid rafts have also exhibited some evidence of compartmentalizing cell adhesion molecules to promote the formation of stable adhesion complexes (Harris et. al., 2001). Lipid rafts exhibit insolubility in non-ionic detergents such as Triton X-100 but can be solubilized by octyl glucoside at 4°C. Due to the high lipid content, they also float to a low density during gradient centrifugation. Many rafts are disrupted by the extraction of cholesterol by reagents such as methyl-β-cyclodextrin, but others show cholesterol independence (Schroeder et. al. 1998; Milhiet et. al. 2001).

GPI-anchored proteins are enriched in lipid rafts because the saturated acyl chains can pack densely with sphingolipids. They are found on the apical surface of polarized epithelial cells, like lipid rafts, and the preferential association of the anchor with sphingolipids might act as a sorting signal. This type of anchor can be found on cells displaying a variety of functions such as signaling, cell adhesion, and enzymatic activity.

Most GPI-anchored proteins are resistant to detergent solubilization by Triton X-100 and are susceptible to cleavage by PI-PLC. AChE of erythrocytes is an exception to both these criteria. It can be solubilized by Triton X-100 and has not been reported to reside in lipid rafts. It also retains an additional acyl chain that is removed in most other GPI-anchored proteins before reaching the cell surface. This renders the protein resistant to PI-PLC cleavage.

Hypothesis and Specific Aims

Preliminary results in our lab indicated that AChE exists as a phospholipase-C sensitive GPI-anchored protein in Caco-2 cells. It was established that most of the cholinesterase activity in this system reflects AChE and not BuChE. It was also found to exist as a globular monomer (Plageman et. al. 2002). My goal was to determine the specific form of AChE and to ascertain whether it is present as a component of lipid rafts. The central hypothesis was that a rare form of AChE is present on the apical surface of Caco-2 adenocarcinoma cells where it exists as a GPI-anchored protein associated with lipid rafts. The specific aims utilized to test this hypothesis were as follows:

Aim 1: Localize AChE to lipid rafts;

Aim 2: Determine the cholesterol dependence of these rafts; and

Aim 3: Identify the AChE splice variants expressed in Caco-2 cells.

MATERIALS AND METHODS

Cell Culture

Caco-2 cells were obtained from American Type Culture Collection (ATCC) at passage 18 and grown in Dulbecco's Modified Essential Medium supplemented with 10% heat inactivated fetal bovine serum (FBS; Atlanta Biologicals, Norcross, GA), 1% non-essential amino acids (MediaTech, Herndon, VA), 1% L-glutamine (MediaTech, Herndon, VA), 100 U/ml penicillin and 100 μg/ml streptomycin (MediaTech, Herndon, VA) at 37°C, 95%O_2, and 5% CO_2 (Pauletti et. al. 1996). In the present studies, cells were used between passages 45 and 60. The cells were maintained in T-75 culture flasks (Corning Inc., Corning, NY) and subcultured when they reached 80%-90% confluency at a split ratio of 1:13. This was done using 0.1% EDTA in PBS, followed by treatment with 0.25% trypsin/0.1% EDTA without Ca^{2+} (MediaTech, Herndon, VA), and cells were then resuspended in fresh DMEM. For experiments, cells were counted using a hemacytometer and usually plated onto 60 mm^2 petri dishes at a density of 60,000 cells per plate. Medium was changed the following day and every 48 hours thereafter.

Assays

Two enzymatic assays were used in the present experiments, including an acetylcholinesterase assay, as well as an assay for alkaline phosphatase. Alkaline phosphatase was assayed because it is a known GPI-anchored protein that is localized to

lipid rafts of brush border membranes. If AChE is actually located in lipid rafts as a GPI-anchored protein, the assay results of AChE should parallel those of alkaline phosphatase. A modified version of the Ellman assay (Ellman et. al., 1961) was used to estimate AChE activity. The assay was performed in 96-well microplates (Falcon, Lincoln Park, N.J.) at a total volume equal to 0.05 ml. Samples were added in volumes of 0.01-0.025 ml with 0.1 M phosphate buffer (pH 8.0) bringing the volume to 0.025 ml. To inhibit any BuChE present, 0.045mM tetraisopropylpyrophosphoramide (iso-OMPA) was added, and blanks were treated with both iso-OMPA and 0.01 mM BW284C51, a specific AChE inhibitor. After a 20-minute room temperature incubation, 0.3 mM dithiobisnitrobenzoic acid (DTNB) was added followed by 1.0 mM acetylthiocholine. Absorbance was measured at 412 nm in a UVmax microplate reader with SOFTmax software v2.01 (Molecular Devices, Menlo Park, CA).

Activity was calculated as IU/L using the following calculation:

$$(\Delta A_{sample}-\Delta A_{blank})/\text{time of assay} \times \text{factor} = IU/L$$

where factor is:

$$(V_t * 10^6)/(E * L * V_s)$$

and V_t = total reaction volume (usually 0.05 ml)

10^6 = conversion factor since E is moles and IU is micromoles

E = extinction coefficient of 1.36×10^4 L/mo/cm

L = path length (determined by volume of a cylinder; $V=\Pi r^2 h$): Diameter of Corning 96-well microplate wells is 0.64 cm. Therefore, for a reaction volume of 0.05 ml, L = 0.15542, neglecting the meniscus.

V_s = sample volume (between 0.01 and 0.025 ml)

Alkaline phosphatase was assayed using a microplate colorimetric assay. Samples were added in volumes of 3-5µl using an alkaline buffer of 1.0 M diethanolamine and 1.0 mM $MgCl_2$ at pH 10.0 to bring the volume up to 95 µl. To initiate the reaction, 5µl of 2.5 mM p-nitrophenyl phosphate (Sigma-Aldrich, St. Louis, MO) was added, and absorbance was read at 412 nm at appropriate time intervals.

Activity was calculated using the following equation:

$$[((\Delta A/\text{time of assay}) * 10^3)/E] * 10^3 * (V_t/V_s) = \text{mU/L}$$

where:

10^3 = conversion factor since E is moles and U is millimoles

E = Extinction coefficient of 1.62×10^4 L/mo/cm

10^3 = conversion factor to express activity in mU versus U

V_t = total reaction volume (usually 0.1 ml)

V_s = sample volume (between 0.003 and 0.005 ml)

In experiments using MβCD, cholesterol was assayed also. The assay used is a modification of the cell homogenate procedure described by Gamble et. al., 1978. Cell homogenate samples of 100 µl were centrifuged and resuspended in 750 µl of 0.1 M potassium phosphate buffer, pH 7.4. Sodium cholate (20 mM in potassium phosphate buffer) containing 1% Triton X-100 was added (20 µl) along with 25 µl of 95% ethanol. Cholesterol oxidase (1 U/ml), peroxidase (10 U/ml), and cholesterol esterase (0.1 U/ml) [Sigma-Aldrich, St. Louis MO] were added in volumes of 111 µl each. *p*-Hydroxyphenylacetic acid at a concentration of 4 mg/ml was added (167 µl). Samples were incubated for one-hour at 37°C and fluorescence was measured on a spectrofluorometer (excitation, 325 nm; emission, 415 nm). Standards (0.1 to 5 µg/750 µl) were made using cholesterol dissolved in 0.1 M potassium phosphate buffer, 95%

ethanol, and sodium cholate by mild heating.

Localization of Acetylcholinesterase

Polarized epithelial cells, such as Caco-2 cells, are known to have a high concentration of sphingolipids on the apical membrane. Therefore, it is hypothesized that lipid rafts would be abundant on the apical surface as well. To determine whether AChE is located on the apical surface, cells were seeded on collagen-coated polycarbonate membranes (Transwell, 3μm pore size, 24.5 mm diameter; Corning Inc., Corning, NY) at a density of 3.75 X 10^5 cells/well. At various time points during culture, trans epithelial electric resistance (TEER) measurements were taken to determine the integrity of the monolayer. On day 22, media was removed and cells were rinsed five times with HBSS in both chambers and then replaced with fresh HBSS. To quantitate AChE activity on the apical membrane, the upper chambers of six wells received 0.045 mM iso-OMPA to inhibit BuChE, and six received 0.045 mM iso-OMPA in addition to 0.01 mM BW284C51 to inhibit both BuChE and AChE. Following a 20-minute incubation, 1mM acetylthiocholine iodide was added to each upper chamber. Samples (0.025 mls) were removed every 15 minutes and added to a solution of 0.3 mM dithiobisnitrobenzoic acid (DTNB), and absorbance was immediately determined. To control for leakage across the cell monolayer, samples were taken from both the upper and lower chambers. The procedure was repeated, but inhibitors and substrate were added to the lower chamber to determine activity on the basolateral membrane.

Cells were then stripped from the membranes by a 15-minute incubation with a

trypsin-free cell stripper (MediaTech, Herndon, VA). The cell suspension was then transferred to a centrifuge tube and washed with HBSS two times by centrifugation at 1,200 rpm for 8 minutes. Following the second centrifugation, cells were resuspended in 1 ml HBSS and counted on a Coulter Counter (Coulter Corporation, Miami, FL). To determine the total amount of AChE per well, the cells were then homogenized and centrifuged at 39,000 rpm, 4°C for 30 minutes as described under detergent solubilization. Pellets were resuspended in 45 mM octyl glucoside in 50 mM Tris HCL with 0.2 mM EDTA and 1 M NaCl and incubated on ice for 20 minutes. Samples were centrifuged again and supernatants assayed for AChE to obtain total activity.

Detergent solubilization and

phosphatidylinositol-specific phospholipase C digestion

Proteins associated with lipid rafts have been found to be resistant to solubilization by Triton X-100 and most other non-ionic detergents at 4°C. In addition, glycosyl phosphatidylinositol-anchored proteins are enriched in lipid rafts. Preliminary experiments in our lab indicated AChE of Caco-2 cells was released from the membrane by treatment with phosphatidylinositol-specific phospholipase C (PI-PLC), and therefore, found in the aqueous phase after ultracentrifugation. To determine if AChE is found in detergent-resistant lipid rafts, Caco-2 cells were seeded onto 60 mm^2 plastic petri dishes at a density of approximately 60,000 cells/plate. On day 15, cells were rinsed 5 times with Hank's Balanced Salt Solution (HBSS; 1.26 mM $CaCl_2 2H_2O$, 0.8 mM $MgSO_4$, 5.36 mM KCl, 0.44mM KH_2PO_4, 136 mM NaCl, 0.337 mM Na_2HPO_4, 5.5 mM D-glucose;

Sigma-Aldrich, St. Louis, MO) to remove culture medium and all traces of serum. They were then gently scraped with a rubber policeman into cold phosphate buffered saline and homogenized with a motorized glass-glass pestle. Homogenates were equally aliquoted into four groups and centrifuged at 39,000 rpm (Ti65 rotor; Beckman LE-80K ultra, Beckman Instrumentation, Palo Alto, CA), 4°C for 30 minutes. Pellets were resuspended in either 1% Triton X-100, 1% Tween 20, 45mM octyl-glucoside, or 5U/ml PI-PLC (*Bacillus cereus;* Sigma-Aldrich, St. Louis, MO). Detergent samples were incubated on ice for 30 minutes, whereas the PI-PLC samples were incubated for 60 minutes at 37°C. Following incubations, samples were again centrifuged at 39,000 rpm, 4°C for 30 minutes. Supernatants were assayed for AChE and alkaline phosphatase.

OptiPrep Gradient Centrifugation

Lipid rafts contain high amounts of sphingolipids and are known to float to a low density during gradient centrifugation. Therefore, the proteins associated with these structures would also be found in the low-density fractions. To further support the hypothesis that AChE exists in lipid rafts, Caco-2 cells were subjected to OptiPrep (60% iodixanol; Axis shield, Oslo, Norway) gradient centrifugation. Cells were seeded onto 60 mm^2 plastic petri dishes at a density of approximately 60,000 cells/plate. On day 15, cells were rinsed 5 times with HBSS to remove culture medium and all traces of serum. They were gently scraped with a rubber policeman into 250 µl of cold phosphate buffered saline (PBS) and homogenized in a Dounce homogenizer with 15 strokes of the pestle. Samples were centrifuged at 39,000 rpm, 4°C for 30 minutes and then resuspended in

250 µl of either PBS alone or 5 U/ml PI-PLC in PBS for one-hour at 37°C. Then, PBS containing Optiprep (50%) and 0.5% Triton X-100 was added (250 µl) to the samples. Triton X-100 was included to solubilize the membrane surrounding lipid rafts. A 10%-40% discontinuous OptiPrep gradient was layered over the 500 µl sample in steps of 10% to equal a total volume of 4.5 ml. The gradients were centrifuged at 4°C, 41,000 rpm for 4 hours (SW 50.1 rotor; Beckman L7-55 ultra, Beckman Instrumentation, Palo Alto, CA). Fractions (250 µl) were collected from the top of the gradient by pipetting and assayed for acetylcholinesterase and alkaline phosphatase.

Depletion of cholesterol with methyl-β-cyclodextrin

Cholesterol is packed tightly between the sphingolipids of lipid rafts, and it has been demonstrated that some rafts can be disrupted by cholesterol extraction. A common method of cholesterol extraction is treatment with methyl-β-cyclodextrin (MβCD). This method was used here to determine if the lipid rafts in which AChE resides are cholesterol dependent. Cells were seeded at a density of 60,000 cells/plate and grown for 15 days. On day 15, DMEM complete media was replaced with serum-free DMEM to rid the cells of exogenous cholesterol. After 18 hours, media was replaced with 100 mM MβCD (Sigma-Aldrich, St. Louis, MO) in serum-free media or serum-free media alone. Following a one-hour incubation at 37°C, cells were rinsed 5 times with HBSS to remove culture medium and all traces of serum.

Plates were then divided into two groups. Each plate from one group was gently scraped with a rubber policeman into 250 µl cold phosphate buffered saline (PBS)

containing 50% OptiPrep and 0.5% Triton X-100. The cells were homogenized in a Dounce homogenizer with 15 strokes of the pestle. A 10%-40% discontinuous OptiPrep gradient in steps of 10% was layered over the 250 μl sample and centrifuged at 4°, 41,000 rpm for 4 hours. Fractions of 250 μl were collected from the top of the gradient and assayed for acetylcholinesterase and alkaline phosphatase. Plates from the second group were scraped into 300 μl PBS and homogenized with a glass-glass motorized homogenizer. Samples (100 μl) were aliquoted to one of two tubes and centrifuged at 39,000 rpm for 30 minutes. Pellets were resuspended in PBS containing either 1% Triton X-100 or 45 mM octyl glucoside and incubated on ice for 20 minutes. Samples were centrifuged again and supernatants assayed for AChE and alkaline phosphatase. The remaining 100 μl was stored at -20°C for a cholesterol assay.

Co-localization of acetylcholinesterase with GM_1

Ganglioside GM_1 is a common lipid raft marker, as well as the receptor for cholera toxin. To establish further evidence of the existence of AChE in lipid rafts, I used fluorescent labeling and microscopy to co-localize GM_1 with AChE. Cells were grown on collagen coated 8-well slides (BioCoat, Becton Dickinson, Franklin Lakes, NJ) at a seeding density of 32,000 cells per well. On day 15, cells were rinsed with 0.2% BSA in PBS followed by a 10 minute block in 0.2% BSA on ice. They were incubated with a mouse monoclonal anti-human AChE antibody, AE2 (gift of R. Rotundo, Miami University, Miami, FL), at 30mg/ml for 2 hours on ice. Cells were washed 3 times, 10 minutes each, in 0.02% BSA. This was followed with a Rhodamine Red conjugated Goat

Anti-Mouse IgG (Jackson Immuno Research, West Grove, PA) at 1:75 and FITC-labeled Cholera Toxin B subunit (Sigma-Aldrich, St. Louis, MO) at 4mg/ml for 1 hour on ice. Cells were washed 3 times for 10 minutes each and fixed with 3.75% Paraformaldehyde for 10 minutes at room temperature. They were rinsed in phosphate buffered saline, mounted, and coverslipped. Slides were viewed using a Nikon PCM 2000 confocal microscope and simple PCI software (Compix, Inc Imaging Systems).

Identification of the acetylcholinesterase splice variants

According to Soreq et. al. (2001), there exists three splice variants of AChE differing in their carboxyl terminus. The messenger RNA (mRNA) of the synaptic form (AChE-S) contains exons 1-6 with exon 5 spliced out. This form is anchored to the membrane by a collagen-like tail or a hydrophobic tail. The mRNA of the erythrocytic form (AChE-E) contains exons 1-5. It is believed that exon 5 allows for the attachment of a GPI-anchor. The third variant, called a readthrough (AChE-R), has exons 1-4 followed by intron 4 which is spliced out in the other two variants. The mRNA also contains exon 5, but it is thought that translation ends at intron 4; so the ability for GPI attachment is lost in the readthrough form; therefore it is believed to exist as a soluble monomer. Contrary to this belief, some investigators have identified mRNA for a GPI-linked, dimer readthrough in several tumor cells (Karpel et. al., 1994). Due to the PI-PLC sensitivity detected in preliminary studies, the AChE-E variant was predicted to be amplified in Caco-2 cells.

To fulfill this specific aim, I extracted RNA from Caco-2 cells using the Trizol method (Invitrogen, Carlsbad, CA). Briefly, cells were lysed in 1.5 ml of Trizol and incubated for 5 minutes at room temperature. Chloroform (0.3 ml) was added and incubated for 3 minutes at room temperature followed by centrifugation at 12,000 rpm for 15 minutes at 4°C in a microfuge. The upper aqueous phase was transferred to a new tube where 0.75 ml of isopropanol was added to precipitate the RNA. The mixture incubated for 10 minutes at room temperature followed by a 10 minute centrifugation at 12,000 rpm at 4°C. The pellet was washed with 1 ml of 75% ethanol, dried, and resuspended in 0.05-0.075 ml DEPC treated water. RNA was quantitated at 260 nm and 4μg was reverse transcribed using reverse transcriptase (Fisher Scientific), Oligo dT (Invitrogen, Carlsbad, CA), dNTP (Fisher Scientific), 5mM magnesium (Fisher Scientific), and RNAse inhibitor (Fisher Scientific). The conditions were as follows: 22°C for 10 minutes, 42°C for 30 minutes, and 95°C for 5 minutes followed by a 4°C chill. Product (4 μl) was amplified using three primer pairs described by Karpel et. al. (1994). The forward primer, 1 (5'-CGGGTCTACGCCTACGTCTTTGAACACCGTGCTTC –3'), amplifies E3. The reverse primers were 2 (5'- CACAGGTCTGAGCAGCGATCCTGCTTGCTG –3'), which amplifies E6 for the synaptic form, 3 (5'- GGTTACACTGGCGGGCTCC –3), to amplify the readthrough transcript, and 4 (5'- ATGGGTGAAGCCTGGGCAGGTG –3') to amplify the GPI-linked transcript. Primers (Integrated DNA Technologies, Coralville, IA) were used at a concentration of 0.01 mg/ml and Taq polymerase (Fisher Scientific) was used at 1:100. GAPDH was also amplified in the samples to ensure equal loading of RNA. A hot start was performed for optimization (Taq was added after the samples

reached 94°C). A step program of 39 cycles was done in an Eppendorf Mastercycler (Brinkmann, Westbury, NY) as follows: 94°C for 2 minutes then denaturation at 94°C for 1minute, annealing at 60°C for 1 minute, and extension at 72°C for 1 minute, followed by 5 minutes at 72°C and a 4°C chill. PCR products were run out on a 2% agarose gel stained with ethidium bromide and viewed in a Nucleovision imager (Nucleotech,Westport, CT). Densitometry was done to qualitatively determine the expression levels of each transcript.

Statistical Analysis

Data was analyzed using SigmaStat (SPSS Inc., Chicago, IL) software and plotted with SigmaPlot. Where applicable, the students T-test was performed with a level of signigicance of $p<0.05$. Solubility studies were analyzed using one-factor analysis of variance (ANOVA), where $p<0.05$.

RESULTS

Localization of Acetylcholinesterase

Acetylcholinesterase activity from the apical and basolateral surfaces of confluent Caco-2 cells grown on Transwells was assayed as described. When samples were taken from the surface to which substrate was added, apical activity was nearly ten times greater than basolateral activity (Figure 7). Samples were also taken from the opposite chamber to control for substrate leakage across the membrane. This activity was insignificant ($n=6$; $p < 0.05$).

Detergent solubilization and phosphatidylinositol-specific phospholipase C digestion

Caco-2 cells were homogenized, centrifuged, and resuspended in various detergents to determine if AChE can be solubilized by non-ionic detergents or if it is only soluble in octyl glucoside. Samples were also treated with 5 U/ml PI-PLC to cleave the GPI-anchor and soluble activity was compared to activity in the detergent-soluble fractions. Activity is expressed in IU/ plate by multiplying IU/L in the 10µl assay volume by 30 to obtain the activity in the total harvest volume of 300 µl/plate. Activity was lowest in the Tween-20 treated samples and increased slightly in samples solubilized by Triton X-100 (Figure 8a). PI-PLC released a significant amount of AChE into the soluble fraction ($n=3$; $p < 0.05$), but octyl glucoside solubilized a significantly greater

amount of enzyme – more than a two fold increase over that of Triton X-100 and a 1.4 fold increase over PI-PLC. Alkaline phosphatase activity was parallel to AChE (Figure 8b).

Optiprep Gradient Centrifugation

Homogenized Caco-2 cells were either untreated or treated with 5 U/ml PI-PLC and subjected to Optiprep density centrifugation as described in Materials and Methods. Fractions were assayed for AChE and activity is expressed in IU/fraction by multiplying IU/L in the 25 μl assay volume by 10 to obtain the activity in the total fraction volume of 250 μl. The greatest activity in untreated samples was found in fractions 14 and 15 near the top of the gradient (Figure 9a). In PI-PLC treated samples, a significantly greater amount of activity was found near fractions 9 and 10 ($n=3$; $p < 0.05$). Alkaline phosphatase was also assayed and showed similar results (Figure 9b).

Figure 7. Localization of AChE to the apical surface. Cells grown on Transwell membranes were assayed for AChE using a modification of the Ellman Assay. Results represent enzyme activity as defined by controls that were inhibited with BuChE and AChE inhibitors. Activity is expressed as means ± S.E.M., n=6. *p < 0.05 indicates a significant difference in apical activity versus basolateral activity by student's t-test.

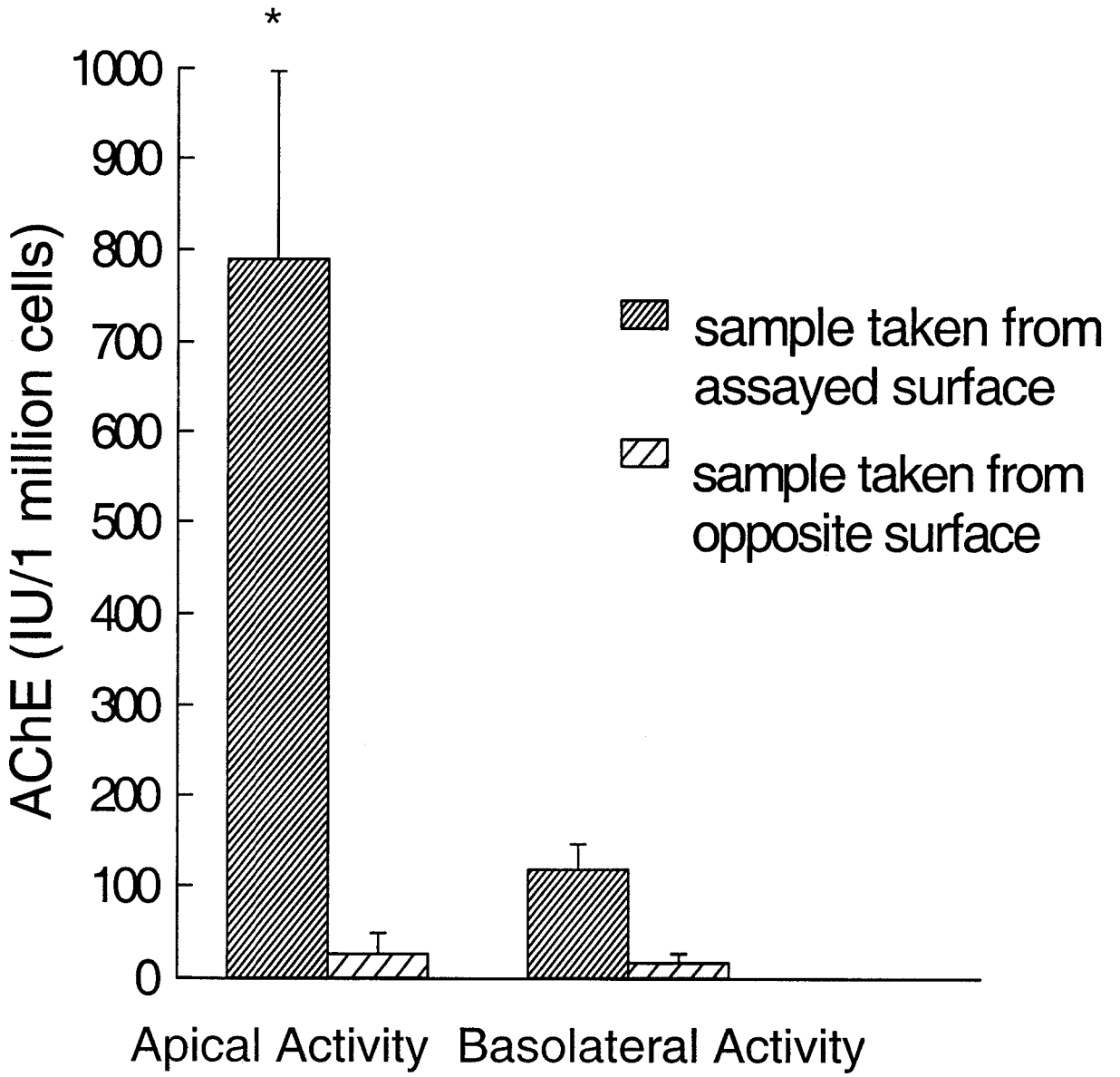

Figure 8. Detergent solubility. Homogenized cells were centrifuged at 4°, 39,000 RPM for 30 min. They were resuspended in various detergents/PBS and incubated for 30 min. at 4° or in PI-PLC/PBS and incubated at 37° for 1 hr. Samples were centrifuged again and supernatants were assayed for AChE (Figure 8a) or alkaline phosphatase (Figure 8b) activity. Data are presented as means ± S.E.M., n=3. *$p < 0.05$ indicates a significant difference in solubilized enzyme as compared to Triton X-100 and Tween 20.

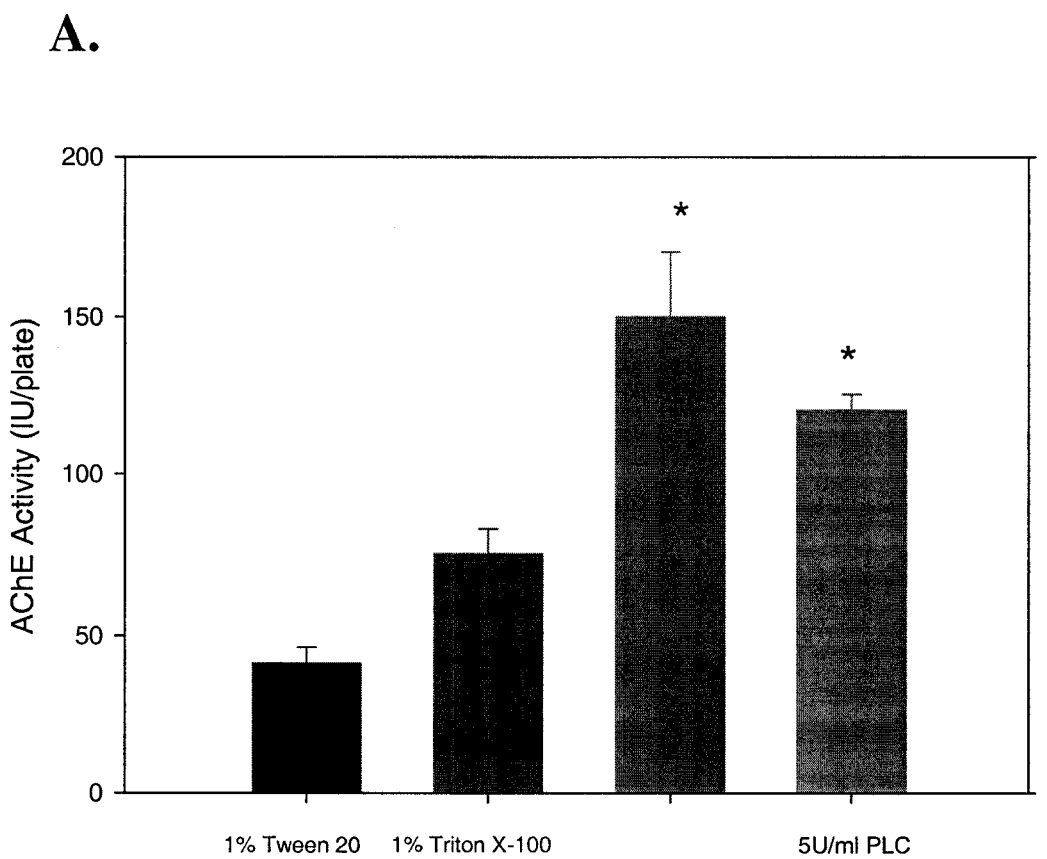

B.

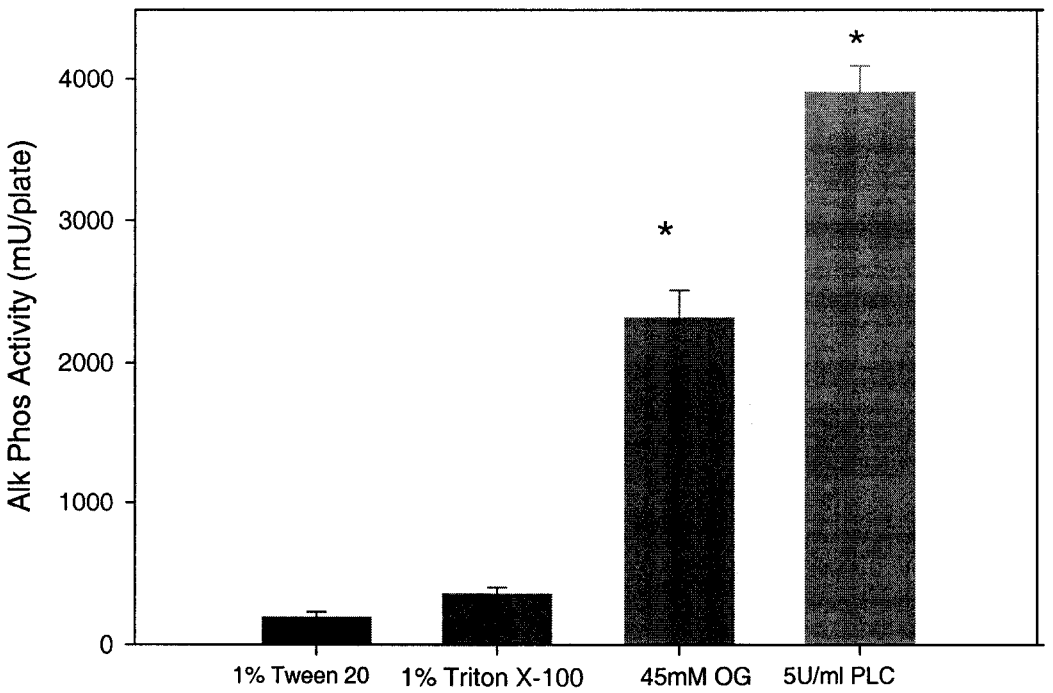

Figure 9. Flotation in a density gradient. Homogenized Caco-2 cells (250 μl) were either untreated or treated with 5 U/ml PI-PLC. Then, 50% OptiPrep with 0.5% Triton X-100 was added (250 μl) and a 10%-40% discontinuous OptiPrep gradient was layered over the sample and centrifuged at 4°, 41,000 RPM for 4 hours. Fractions (250 μl) were collected from the top and assayed for AChE (Figure 9a) or alkaline phosphatase (Figure 9b). Activity is expressed as means ± S.E.M., n=3. *$p < 0.05$ indicates a significant difference between groups. Fraction 1 is the bottom of the gradient (most dense) while fraction 18 is at the top (least dense).

A.

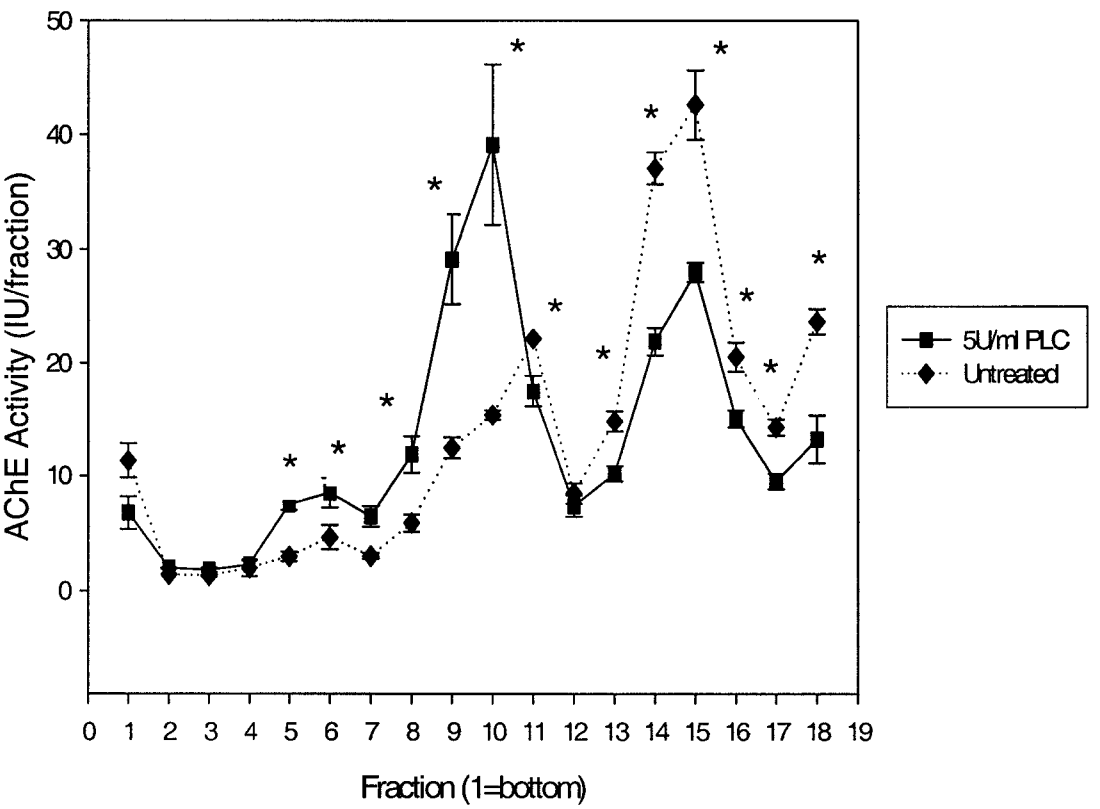

B.

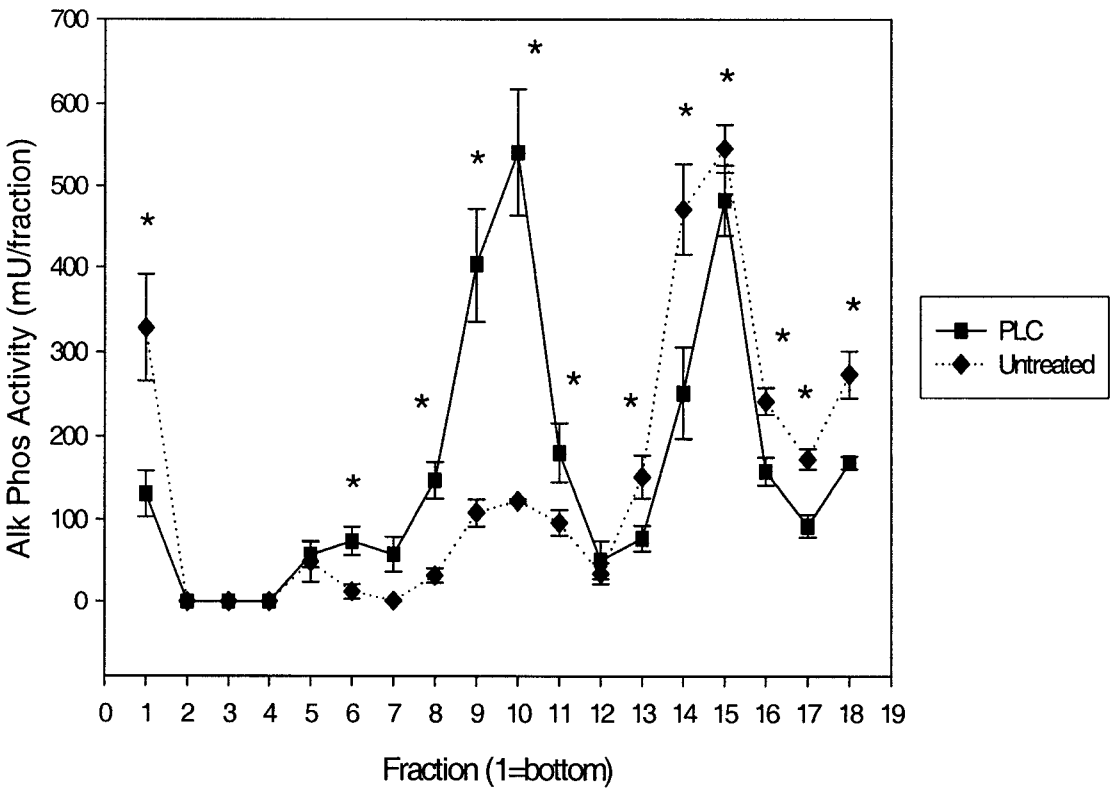

Depletion of cholesterol with methyl-β-cyclodextrin

Cholesterol was depleted in Caco-2 cells by treatment with 100mM MβCD for one-hour in serum-free media as outlined in Materials and Methods. The plates were then divided evenly into two groups. One group was designated for use in a detergent solubilization experiment and the other group was to be used in an Optiprep gradient centrifugation. Cells were homogenized and appropriately treated as above, according to which group they were in. Small samples of the cell homogenate were taken for use in a cholesterol assay. AChE activity is expressed as IU/plate as described above. Cells that were solubilized in octyl glucoside showed significantly greater AChE activity than those solubilized in Triton X-100 for both untreated and MβCD treated samples (Figure 10a). There was no significant difference in the amount of enzyme solubilized by Triton X-100 in the treated samples versus the untreated samples ($n=3$; $p < 0.05$). Alkaline phosphatase activity paralleled these results (Figure 10b). A cholesterol assay on these samples showed more than a 60% reduction of cholesterol in the MβCD treated samples as compared to the untreated samples (Figure 10c).

The group designated for Optiprep gradient centrifugation showed a significant peak in AChE activity in fractions 14 and 15 in untreated samples (Figure 11a) [$n=3$; $p < 0.05$]. Samples treated with MβCD showed the greatest activity in fractions 12,13, and 14. Again, activity is expressed as IU/fraction as done above. An alkaline phosphatase assay of the fractions resulted in similar peaks of activity (Figure 11b). Cholesterol in the treated samples was reduced by nearly 80% as compared to untreated samples (Figure 11c).

Figure 10. Detergent solubility after MβCD treatment. Cells were cultured in serum-free DMEM for 18 hours and then replaced with 100mM methyl-β-cyclodextrin. Cells were then homogenized in PBS and centrifuged at 4°, 39,000 rpm for 30 min. They were resuspended in either 1% Triton X-100 or 45 mM octyl glucoside in PBS and incubated for 30 min. at 4°. Samples were centrifuged again and supernatants were assayed for AChE (Figure 10a) or alkaline phosphatase (Figure 10b) activity. Data are presented as means ± S.E.M., n=5. *$p < 0.05$ indicates a significant difference in enzyme solubilized by octyl glucoside versus Triton X-100. Cholesterol was assayed using a modified version of Gamble et. al. (1978) (Figure 10c). Results are expressed as cholesterol remaining in percent mean of untreated samples.

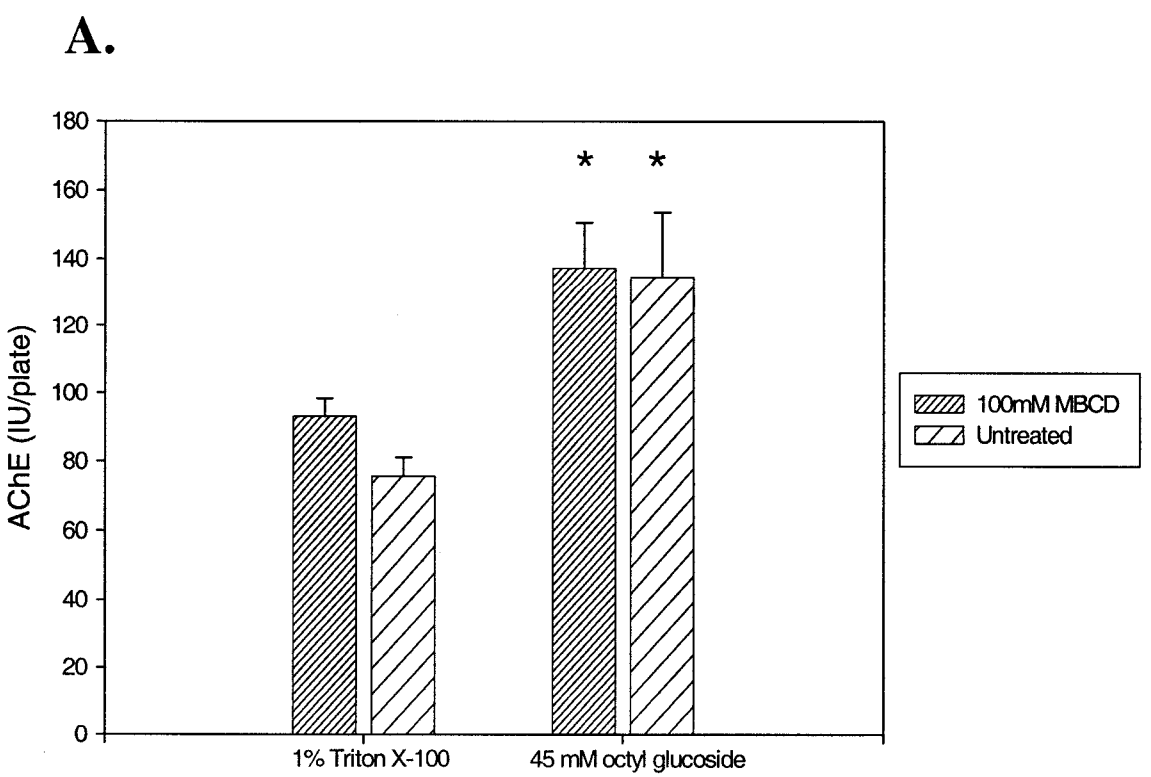

B.

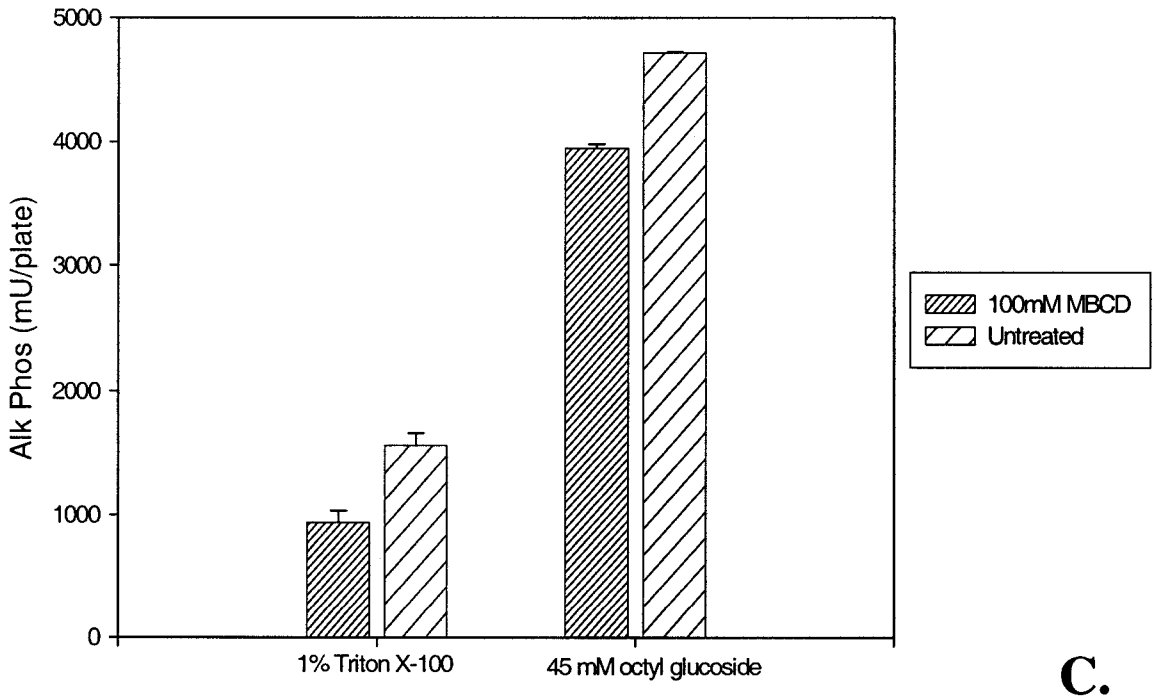

C.

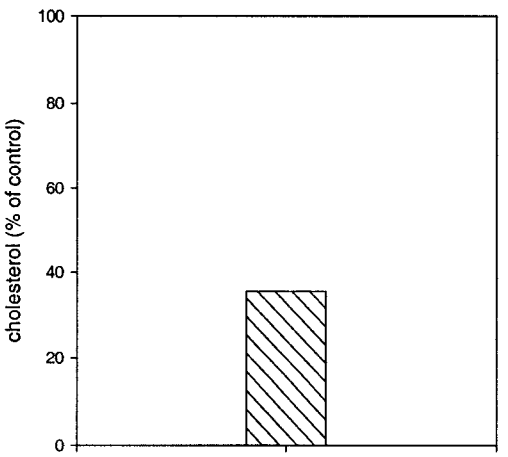

Figure 11. Flotation in a density gradient after MβCD treatment. Cells were cultured in serum-free DMEM for 18 hours and then replaced with 100mM methyl-β-cyclodextrin. The plates were incubated for 1 hour at 37° and homogenized in PBS containing 50% Optiprep and 0.5% Triton X-100 (250 μl). The samples were layered under a 10-40% OptiPrep gradient and centrifuged at 4°, 41,000 rpm for 4 hours. Fractions (250 μl) were collected from the top and assayed for AChE (Figure 11a) or alkaline phosphatase (Figure 11b). Activity is expressed as means ± S.E.M., n=3. *$p < 0.05$ indicates a significant difference between groups. Fraction 1 is the bottom of the gradient (most dense) while fraction 18 is at the top (least dense). Cholesterol was assayed using a modified version of Gamble et. al. (1978) (Figure 11c). Results are expressed as cholesterol remaining in percent mean of untreated samples.

A.

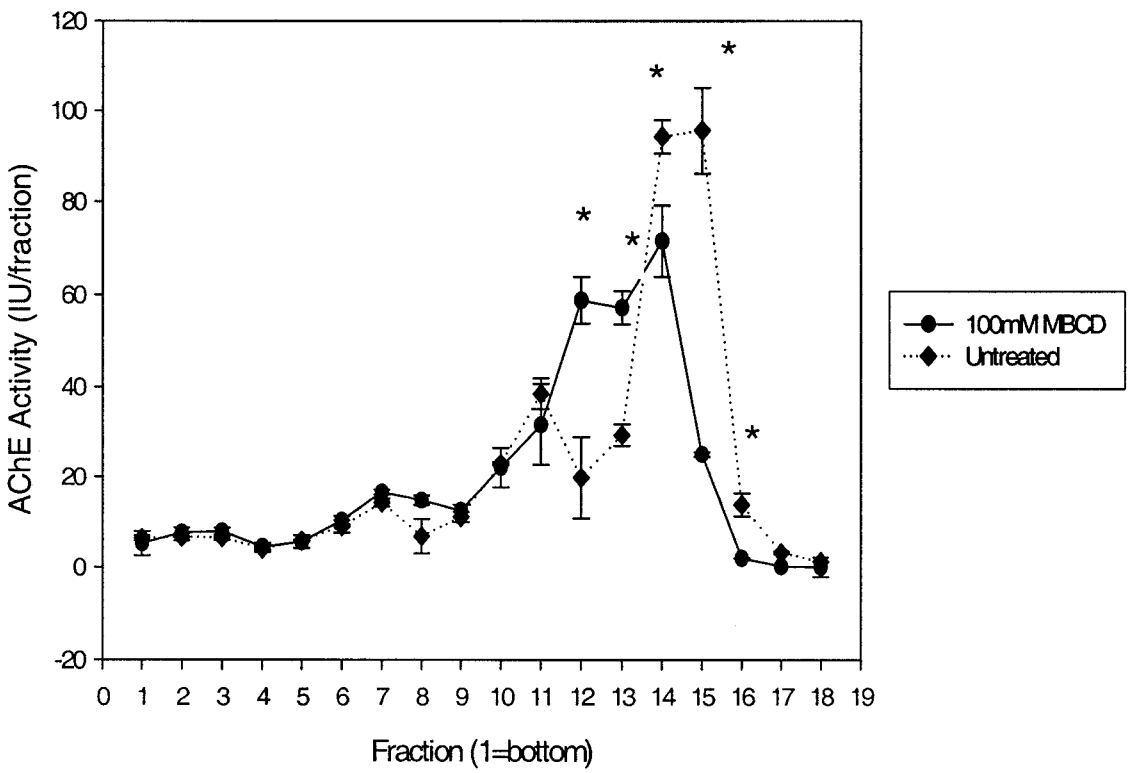

B.

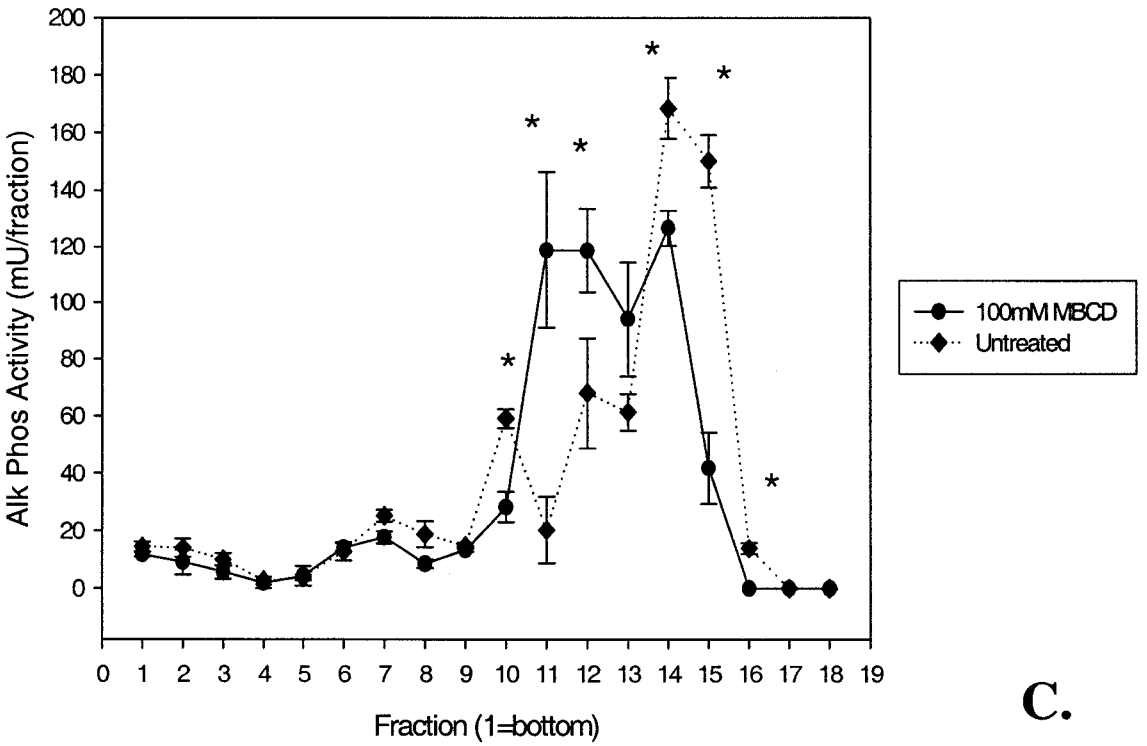

C.

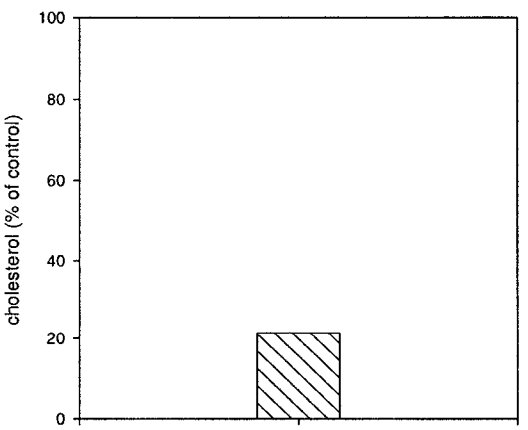

Co-localization of acetylcholinesterase with GM_1

Caco-2 cells grown on collagen-coated slides were treated with an anti-AChE antibody as described in Material and Methods. A Rhodamine-conjugated secondary antibody and FITC-conjugated cholera toxin B subunit were then added. Slides were viewed with a confocal microscope to determine co-localization of AChE and the ganglioside GM_1. Figure 12a shows GM_1 staining alone and Figure 12b shows only AChE staining. Patching of these proteins in the membrane is evident in both photographs. Figure 12c is an overlay of GM_1 and AChE staining. Arrows identify yellow patches where AChE is co-localized with GM_1 in lipid rafts.

Identification of the acetylcholinesterase splice variants

Total RNA from Caco-2 cells was extracted and quantitated. The RNA was reverse transcribed and then amplified by PCR. Three primer pairs were used to detect three alternative AChE splice variants. Primers one and two (see Materials and Methods) amplify exon 6 (Figure 13b) to give rise to a 481 base pair transcript, which is the major form in brain and muscle (AChE-S). Primers one and three amplify the region containing intron 4, found only in the readthrough form (AChE-R), to obtain a 418 base pair product. The primer pair of one and three amplifies exon 5, enabling the addition of a GPI-anchor (AChE-H), to produce a 396 base pair transcript. The products were run out on an agarose gel stained with ethidium bromide and viewed by an ultraviolet imager.

Figure 13a reveals the presence of three AChE mRNA species. Comparative densitometric analysis revealed the dominant species to be AChE-S and AChE-E. The

band reflecting the readthrough (AChE-R) transcript was considerably less intense (more than a two-fold difference) and may indicate a relatively low abundance of this mRNA. The RT-PCR was performed on three separate samples of Caco-2 cells. All three transcripts were amplified in each sample, although densitometric analysis could not be done on all due to saturation. Samples not containing reverse transcriptase were also included (not shown here) and revealed no contamination.

Figure 12. Co-localization of AChE with GM_1. Cells grown on slides were incubated with a monoclonal anti-AChE antibody (AE2) for two hours on ice as described in Materials and Methods. It was followed with a Rhodamine red-conjugated secondary antibody as well as FITC-labeled Cholera Toxin B subunit at for one hour on ice. Cells were washed and fixed with 3.75% Paraformaldehyde and viewed with a confocal microscope. a) GM_1 labeling with Cholera Toxin only; b) Anti-AChE antibody followed by Rhodamine only; c) Overlay. Yellow patches and arrows indicate co-localization of AChE and GM_1 in lipid rafts.

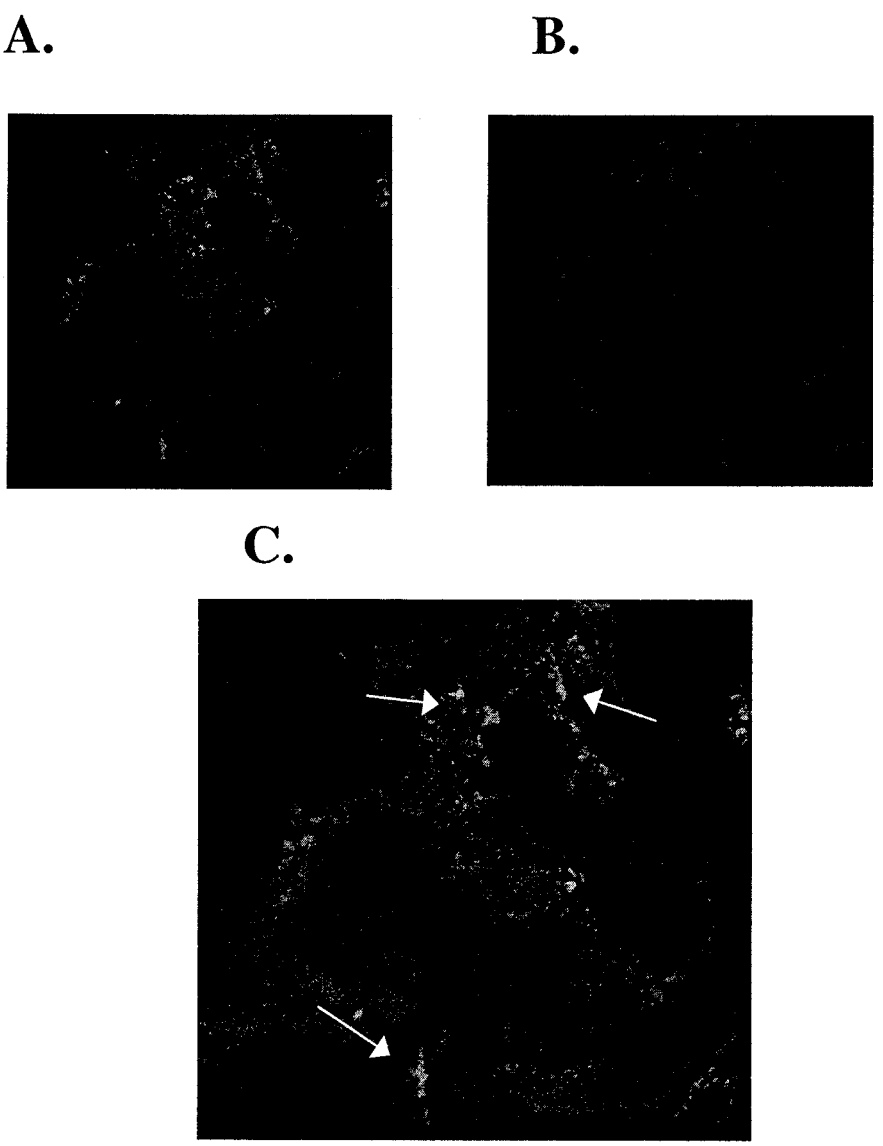

Figure 13.Identification of AChE splice variants. a) Total RNA was extracted by the Trizol method (Invitrogen) and 4μg was reverse transcribed. Product was amplified using three primer pairs as described in Materials and Methods. Lane 1 was amplified using primers for AChE-S (481bp). Lane 2 represents AChE-R (418bp), and lane 3 is AChE-H (396bp). b) AChE gene illustrating the three transcripts and specific primers.

A.

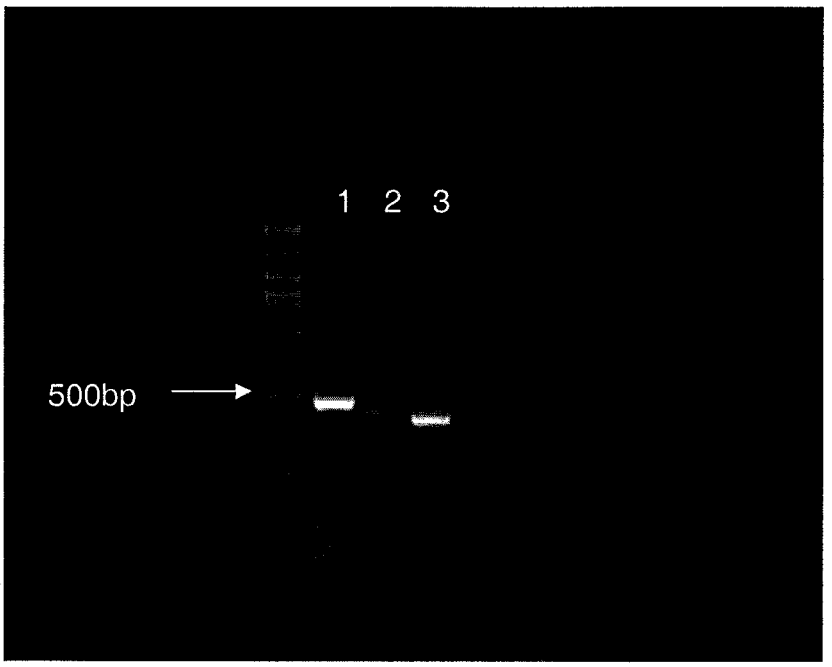

B.

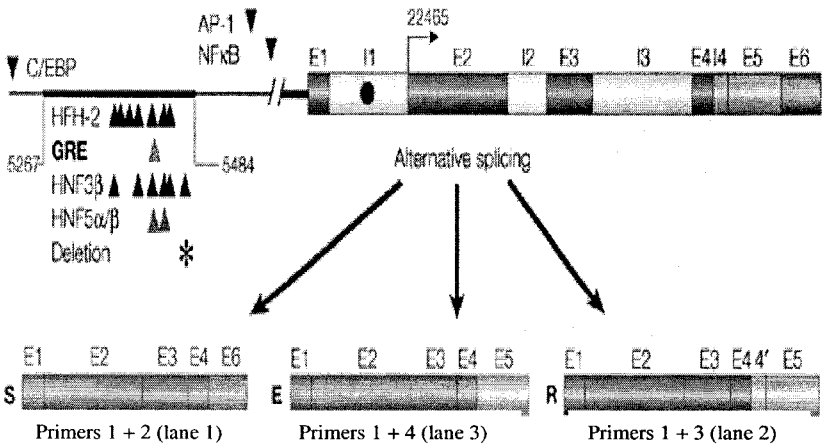

Soreq et. al., 2001

DISCUSSION

AChE exists in multiple isoforms differing in the carboxy terminal sequence, reflecting alternate splicing from a single gene. The mechanism of membrane anchoring differs in each of these variants. As reported by Soreq et. al. (2001), the synaptic form, AChE-S, is anchored to the membrane by a collagen-like tail or a hydrophobic subunit at the neuromuscular junction and in the brain. AChE-E (erythrocytic) is anchored to the membrane by a GPI-moiety in human erythrocytes. The most recently reported form, AChE-R (readthrough) is expressed in response to stress as a soluble protein in the brain. This, and the existence of AChE in several cells outside of the nervous system, is an indication that it may function in some non-classical or non-enzymatic ways. AChE was found in the Caco-2 cell line (Plageman et. al., 2002) and preliminary studies suggested that it was attached to the membrane by a GPI-anchor.

Caco-2 cells are derived from a human adenocarcinoma and are widely utilized as a model of intestinal epithelia. They spontaneously differentiate to form a polarized monolayer. The apical surface is in contact with the media and represents the lumen of the intestine, while the basolateral membrane is involved in cell adhesion. The apical membrane is enriched in constituents of lipid rafts, such as sphingolipids (van't Hof and van Meer, 1990) and GPI-anchored proteins (Garcia et. al., 1993). The present work localized AChE to the apical surface of Caco-2 cells. An assay of each surface of the confluent monolayer demonstrated a six fold higher level of AChE activity on the apical membrane compared to that observed on the basolateral surface.

AChE was found to reside within a detergent-resistant membrane of Caco-2 cells, a common characteristic of GPI-anchored proteins. Octyl glucoside was found to

solubilize 3.5 fold more enzyme compared to Tween 20 and nearly 2.5 fold more than Triton X-100 or Brij 96 (data for Brij 96 not shown). Alkaline phosphatase, a known GPI-anchored protein that resides in lipid rafts of Caco-2 cells, exhibited similar solubility characteristics. These observations confirm those of Garcia et. al. (1993) who also demonstrated these characteristics for alkaline phosphatase in Caco-2 cells. Several previous studies characterized the detergent-resistant domains of Caco-2 cells (Mirre et. al., 1996; Alfalah et. al., 2002; Sapin et. al., 2002). Mirre et. al. (1996) showed that the microdomains did not contain caveolin, a protein required to form flask-shaped invaginations called appear to be lipid rafts.

Results from the experiments showed that treatment with PI-PLC significantly increased soluble AChE activity compared to solubilization in Triton X-100. This suggests that the AChE form present in Caco-2 cells is GPI-anchored and likely differs from the GPI-anchored erythrocytic AChE. The latter contains an additional acyl chain rendering it resistant to cleavage by PI-PLC. The data revealed significantly less enzyme activity when treated with PI-PLC than when solubilized in octyl glucoside. This is attributed to below optimal conditions. Incubation times and concentrations of PI-PLC were not optimized in these studies so it is possible that cleavage of the GPI-anchor would release more than what is solubilized in octyl glucose.

Density centrifugation is a common method of identifying components of lipid rafts (Simons and Toomre, 2000). The high concentration of glycosphingolipids found in rafts results in a tendency to float to a low-buoyant density in a gradient. Caco-2 cells were subjected to Optiprep density centrifugation and AChE was found floating in the low-density fractions, along with alkaline phosphatase. When cells were treated with PI-

PLC prior to Optiprep density centrifugation, a significant amount of AChE shifted to the higher density fractions. Cleavage of the GPI-anchor allows for the release of AChE from the membrane and, therefore, from the low-density rafts. The control GPI-anchored protein, alkaline phosphatase, was also released and found at a higher density.

Lipid rafts are generally believed to be cholesterol-dependent and are often disrupted by the extraction of cholesterol. Common agents used to deplete membrane cholesterol include methyl-β-cyclodextrin, a large carbohydrate molecule that contains a cholesterol-binding pocket (Simons and Toomre, 2000), and saponin, which is used to sequester cholesterol from other areas in the cell. Alfalah et. al. (2002) used 50 mM MβCD to deplete cholesterol from the membrane of Caco-2 cells. The sorting behavior and detergent solubility of dipeptidyl peptidase IV (DPPIV) was then studied. As discussed above, DPPIV was mis-sorted to the basolateral membrane and was recovered in the Triton X-100 detergent-soluble fraction.

It has been demonstrated, though, that some lipid rafts can remain as stable microdomains even after the depletion of cholesterol (Hansen et. al., 2001; Schroeder et. al., 1998; Milhiet et. al., 2002). The current work has suggested that AChE resides in cholesterol-independent lipid rafts. When cholesterol was depleted by more than 70 percent with 100 mM MβCD, AChE was consistently found in the floating fractions of an Optiprep gradient. There was a slight shift in the peak of enzyme activity in MβCD treated samples from fractions 14 and 15 to fractions 12, 13, and 14. The same behavior was observed with alkaline phosphatase. This slight increase in density might reflect the depletion of cholesterol from the lipid domains. Overall activity in treated samples also decreased; this is attributed to the death of some cells from the toxic effects of MβCD.

When cholesterol was depleted by more than 65 percent, no change in detergent solubility was observed. A significant amount of AChE remained insoluble in Triton X-100. Similar results were obtained for alkaline phosphatase.

The concentration of MβCD used in these studies was 10 fold greater than what has been used in other studies demonstrating up to a 70 percent depletion of cholesterol and the disruption of lipid rafts (Harder et. al., 1998; Hao et. al., 2001). Preliminary studies were done using a range of concentrations from 1 mM to 100 mM showing no effect on the flotation or detergent solubility of AChE and alkaline phosphatase (data not shown). Saponin was also used to sequester cholesterol with no significant change in AChE or alkaline phosphatase solubility (data not shown). Similar results were obtained when Garcia et. al. (1993) attempted to disrupt lipid rafts of Caco-2 cells using the cholesterol sequestering agents Nystatin and Digitonin. Neither treatment was found to increase the Triton X-100 solubility of three GPI-anchored proteins studied, including alkaline phosphatase.

One way to analyze lipid raft proteins is by co-localization with known raft-associated markers. This can be done by crosslinking the proteins of interest with antibodies followed by fluorescence-labeled secondary antibodies and immunofluorescence confocal microscopy. Some raft markers can be visualized with fluorescence labeled toxins. Kovbasnjuk et. al. (2001) studied the co-localization of the Shiga toxin receptor, Gb_3, and the lipid raft-associated Cholera toxin, GM_1, in Caco-2 cells using fluorescence labeling. The two receptors were observed to co-localize on the apical surface of Caco-2 cells. Analysis showed that on average 97 percent of labeled Gb_3 co-localized with labeled GM_1. They attempted to disrupt the lipid rafts by treating

the cells with 100 mg/ml MβCD, which is approximately 76 mM. Confocal images showed the same pattern of co-localization between the two receptors as seen in untreated cells; on average, 88 percent of Gb_3 was co-localized with GM_1. The investigators did observe a decrease in the internalization of Shiga toxin but no change in the binding of either toxin to their respective receptors. A decrease in internalization of Cholera toxin was also observed after treatment with 100 mg/ml 2-hydroxy-β-cyclodextrin, another sterol-binding agent (Orlandi and Fishman, 1998). Unlike the former experiment, this group also reported an increase in Triton X-100 detergent solubility as well as a shift from low-density fractions to high-density fractions of GM_1. These results suggest that cholesterol is necessary for the internalization of Shiga toxin and Cholera toxin but not always for the stability of lipid rafts. It is possible that Gb_3 and GM_1 are associated with rafts containing slight differences in sphingolipid to cholesterol ratios so one is dependent on cholesterol while another can exist without cholesterol.

When Harder et. al. (1998) labeled alkaline phosphatase and the raft-associated transmembrane protein, influenza virus hemagglutinin (HA) in non-polarized, fibroblastoid BHK 21 cells, these two proteins were found to overlap extensively. They then labeled alkaline phosphatase along with a non-raft protein, low-density lipoprotein receptor (LDL-R) and observed a clear segregation. Because the co-patching of alkaline phosphatase and HA is predicted to occur through a common lipid preference, they studied the patching behavior of ganglioside GM_1 with alkaline phosphatase and the non-raft marker, human transferrin receptor (hTfR). This was done in Jurkat cells transiently expressing alkaline phosphatase and hTfR, because BHK cells contain amounts of GM_1 too low to be detected by fluorescence-labeled cholera toxin B subunit. They observed

extensive overlapping of alkaline phosphatase and GM_1, as well as a definite exclusion of hTfR from the lipid domains.

The co-localization of AChE with GM_1 was studied. AChE was visualized with a monoclonal antibody followed by a fluorescence-labeled secondary antibody. GM_1 was labeled with FITC-conjugated cholera toxin B subunit. When the proteins were analyzed individually, distinct patches were observed. The brightest patches were found to overlap in the dual image. The co-localization was expected to be more significant, but the FITC tended to fade rapidly during visualization with the confocal microscope.

Valero and Vidal (1995) presented evidence that the AChE expressed in human meningioma contains a GPI anchor that is susceptible to cleavage by PI-PLC. They also reported a monomeric and a dimerized form by sedimentation analysis and found that the dimers were less sensitive to cleavage by PI-PLC and therefore, resembled the erythrocytic form. RT-PCR of extracted RNA from astrocytomas and brain melanomas revealed transcripts for both AChE-S and AChE-R, but the AChE-S protein was the only one to be retained in the astrocytic tumor cells (Perry et. al., 2002). They also observed a shift in splicing from AChE-S to AChE-R, which corresponded to an increase in tumor aggressiveness. These investigators also transfected glioblastoma cells with AChE-R expression vectors. When AChE-R was over-expressed, a significant increase in cell proliferation was seen; whereas cells transfected with only AChE-S showed no significant increase. It is possible that AChE-R promotes proliferation in astrocytomas but is rapidly degraded and cannot be detected.

In the present studies, PCR primers from each of the variable splice domains were used on reversed-transcribed cDNA preparations from Caco-2 cells. The major transcript

in brain and muscle, from which the I4 and E5 domains are spliced, was found. As predicted, the presence of a form containing the E5 domain, conferring GPI-linkage, was confirmed. Interestingly, the unspliced I4 readthrough transcript was also observed. This form is reported to exist as a soluble monomer (Soreq and Seidman, 2001), although earlier published data by the same group (Karpel et. al., 1994) suggested that AChE-R might have the capacity for GPI linkage in some tumor cells. This study on human tumor cell lines revealed the existence of the three transcripts found in the Caco-2 cell line, in addition to a fourth variant. This was detected with the same primer pair that amplified the GPI-linked AChE, but gave rise to a 474 base pair product reflecting a GPI-linked readthrough form. They presented no evidence, though, of protein expression. It was also mentioned that in both the mouse and the rat AChE genes the I4 domain contains a termination codon, and a protein lacking the potential for linkage is produced. Therefore, although message for a GPI-anchor exists, it may not be transcribed.

In the study on Caco-2 cells, only one band was observed when the primer pair amplifying the E5 region was employed. Therefore, it appears that the unique form found by Karpel et. al. (1994) is not present. It was unexpected to find the I4 region amplified in the Caco-2 cDNA samples, because there has been no evidence indicating the existence of secreted AChE (data not shown). It could be a similar case as that proposed above by Perry et. al. (2002) in astrocytic tumors; protein is produced but it is so rapidly degraded that it is undetectable. On the other hand, the mRNA for this readthrough transcript might not be translated into protein.

The current work establishes the existence of a GPI-anchored form of AChE on the apical surface of Caco-2 cells. It is enriched in detergent-resistant, low-density

microdomains similar to those in which alkaline phosphatase is located, and these microdomains appear to be cholesterol-independent. The enzyme is also co-localized in patches with the lipid raft marker, ganglioside GM_1. Furthermore, it was determined that three alternatively spliced mRNAs are expressed in Caco-2 cells. The primary form of brain and muscle, as well as a GPI-anchored variant, are the predominant transcripts. A readthrough form containing intron 4, is produced at significantly reduced levels.

Further investigation is required to determine which proteins are expressed. Studies here indicate that a PI-PLC sensitive enzyme exists, and it is possible that the tailed synaptic form is also expressed. That would explain the activity seen in samples solubilized with Triton X-100 or Tween 20. It would also account for the small peak of activity seen in untreated samples in non-raft fractions 9, 10, and 11 of the Optiprep gradient (Figure 9a). Analysis on the readthrough form is necessary. Perry et. al. (2002) used an antibody targeted at ARP, the C-terminal peptide of the AChE-R protein, to visualize its localization. The protein was not detected in astrocytomas, but they did observe intense staining in metastatic brain melanoma tumors. A similar study could be conducted in Caco-2 cells, or the antibodies could possibly be used for Western blotting.

It would also be necessary to determine the function of AChE in Caco-2 cells. Studies would need to be conducted on normal enterocytes to determine if AChE is present in these cells as well. A study by Sine et. al. (1991) identified AChE in human intestinal cells obtained by scraping. The results should be interpreted with caution, because it would be very difficult to isolate epithelial cells, and scrapings would result in heterogeneous populations. The scrapings likely contained cells from the underlying muscle tissue, which would contain AChE of the neuromuscular junction. Therefore,

normal enterocytes specifically would need to be isolated and studied for the presence of AChE.

There are several known non-neuronal cholinergic systems functioning in epithelial cells, such as keratinocytes and bronchial epithelial cells. It is possible that such a system is present in intestinal epithelial cells where it might be involved in the secretion of ions, water, and macromolecules and in the regulation of ciliary activity as proposed by Wanner et. al. (1996) in bronchial epithelial cells. Other possibilities include cell attachment and inflammatory actions. There is evidence that nicotine suppresses inflammation related to ulcerative colitis in the lining of the large intestine. This may be a result of a functioning non-neuronal cholinergic system. Western blots could be done to detect muscarinic or nicotinic receptors, and HPLC could be utilized to detect ACh. In additon, the AChE synthesizing enzyme, choline acetyl transferase, should be investigated.

It would be interesting to disrupt the synthesis of sphingolipids in an attempt to weaken lipid rafts and determine if this affects the detergent-solubility of AChE or its tendency to float in a gradient. Another possibility is to prevent the synthesis of or the attachment of the GPI-anchor to AChE to determine if it is critical for the function of the enzyme in Caco-2 cells. Other future studies include overexpression of the alternative forms in Caco-2 cells to gain insight into their individual functions or to use anti-sense RNA to knock out the production of AChE and observe the effects on growth and differentiation. This work presents the first evidence of GPI-anchored AChE existing in lipid rafts. In addition, it is the first report of GPI-linked, raft-associated AChE in Caco-2 cells. It is an important contribution to the research on AChE, as well as lipid rafts, and

will hopefully further the understanding of possible non-classical roles of AChE and the function of lipid rafts.

REFERENCES

Alfalah, M., Jacob, R., Naim, HY. Intestinal dipeptidyl peptidase IV is efficiently sorted to the apical membrane through the concerted action of N- and O-glycans as well as association with lipid microdomains. J. Biol. Chem. 277(12):10683-10690, 2002.

Arredondo J. Hall, L.L., Ndoye, A., et. al. Muscarinic acetylcholine receptors regulating cell cycle progression are expressed in human gingival keratinocytes. J. Periodont. Res., 38: 79-89, 2003.

Brown, D.A. and London, E. Functions of lipid rafts in biological membranes. Annu. Rev. Cell Dev. Biol., 14:112-136, 1998.

Brown, Deborah. Structure and function of membrane rafts. Int. J. Med. Microbiol., 291:433-437, 2002.

Cattaneo, M.G., Datri, F., Vicentini, L. M. Mechanisms of mitogen-activated protein kinase activation by nicotine in small-cell lung carcinoma cells. Biochem. J., 328:499-503, 1997.

Chatterjee, S. and Mayor, S. The GPI-anchor and protein sorting. Cell. Mol. Life Sci., 58:1969-1987, 2001.

Darboux, I., et. al. The structure-function relationships in *Drosophila* neurotactin show that cholinesterasic domains may have adhesive properties. EMBO J., 15:4835-4843, 1996.

Deutsch, Varda R., Pick, Marjorie, Perry, Chava, et. al. The stress-associated acetylcholinesterase variant AChE-R is expressed in human $CD34^{+}$ hematopoietic progenitors and its C-terminal peptide ARP promotes their proliferation. Exp. Hematology, 30:1153-1161, 2002.

Dustin, Michael L., Selvaraj, Periasamy, et. al. Anchoring mechanisms for LFA-3 cell adhesion glycoprotein at membrane surface. Nature, 329:846-848, 1987.

Ellman, George L., Courtney, Diane, et. al. A new and rapid colorimetric determination of acetylcholinesterase activity. Biochem. Pharmacology, 7:88-95, 1961.

Falugi, C. and Raineri, M. Acetylcholinesterase and pseudocholinesterase activity and distribution patter in early developing chick limbs. J. Embryol. Exp. Morph. 86:89-108, 1985.

Gamble, W., Vaughan, M., et. al. Procedure for determination of free and total cholesterol in micro- or nanogram amounts suitable for studies with cultured cells. J. of Lipid Res., 19:1068-1070, 1978.

Grando, S.A., Crosby, A.M., et. al. Agarose gel keratinocyte outgrowth system as a model of skin reepithelization: requirement of endogenous acetylcholine for outgrowth initiation. J Invest. Dermatol., 2: 41-48, 1993.

Hansen, Gert H., Immerdal, Lissi, et. al. Lipid rafts exist as stable cholesterol-independent microdomains in the brush border membrane of enterocytes. J. Biol. Chem., 276(34):32338-32344, 2001.

Hao, M., Mukherjee, S., Maxfield, F. Cholesterol depletion induces large scale domain segregation in living cell membranes. PNAS, 98(23):13072-13077, 2001.

Harder, Thomas, Scheiffele, Peter, et. al. Lipid Domain Structure of the Plasma Membrane Revealed by Patching of Membrane Components. J. Cell Biol. 141, 4:929-942, 1998.

Harris, T.J.C., Awrey, D.E., Cox, B.J., et. al. Involvement of a triton-insoluble floating fraction in *Dictyostelium* cell-cell adhesion. J. Jiol. Chem., 274:18640-18648, 2001.

Hooper, N. M. Glycosyl-phosphatidylinositol anchored membrane enzymes. Clin. Chim. Acta, 266:3-12, 1997.

Ilangumaran, Subburaj, Arni, Stephan, et. al. Microdomain-dependent regulation of Lck and Fyn Protein-Tyrosine Kinases in T lymphocyte plasma membranes. Mol. Biol. of the Cell, 10:891-905, 1999.

Karpel, Rachel, Aziz-Aloya, Revital Ben, et. al. Expression of three alternative acetylcholinesterase messenger RNAs in human tumor cell lines of different tissue origins. Experimental Cell Res., 210:268-277, 1994.

Kovarova, Martina, Tolar, Pavel, et. al. Structure-function analysis of Lyn kinase association with lipid rafts and initiation of early signaling events after Fcε receptor I aggregation. Mol. Cell. Biol., 21: 8318-8328, 2001.

Kovbasnjuk, O., Edidin, M., and Donowitz, M. Role of lipid rafts in Shiga toxin 1 interaction with the apical surface of Caco-2 cells. J. Cell Sci., 114:4025-4031, 2001.

Krejci, E., Deval, N., et. al. Cholinesterase-like domains in enzymes and structural proteins: functional and evolutionary relationships; identification of a catalytically essential aspartic acid. Proc. Natl. Acad. Sci., USA 88:6647-6652, 1991.

Kryger, G. et al. Structures of recombinant native and E202Q mutant human acetylcholinesterase complexed with the snake-venom toxin fasciculin-II. Acta Crystallogr. D. Biol. Crystallogr., 56:1385-1394, 2000.

Layer, P. G. Comparative localization of acetylcholinesterase and pseudocholinesterase during morphogenesis of the chicken brain. Proc. Natl. Acad. Sci. U.S.A., 80:6413-6417, 1983.

Massoulié, J., Pezzementi, L., et. al. Molecular and cellular biology of cholinesterases. Prog. Neurobiol., 41:31-91, 1993.

Massoulié, Jean, Anselmet, Alain, Bon, S., et. al. The polymorphism of acetylcholinesterase: post-translational processing, quaternary associations and localization. Chemico-Biol. Interactions, 119-120:29-42, 1999.

Meshorer, Eran, Erb, Christina, et. al. Alternative splicing and neuritic mRNA translocation under long-term neuronal hypersensitivity. Science, 295:508-512, 2002.

Milhiet, Pierre E., Giocondi, Marie-Cecile, and Grimellec, Christian Le. Cholesterol is not crucial for the existence of microdomains in kidney brush-border membrane models. J. Biol. Chem., 277, 2:875-878, 2002.

Mirre, C., Monlauzeur, M., Garcia, M., et. al. Detergent-resistant membrane microdomains from Caco-2 cells do not contain caveolin. Am. J. Physiol., 271:C887-C894, 1996.

Oh, Phil and Schnitzer, Jan E. Segregation of heterotrimeric G proteins in cell surface microdomains. Mol. Biol. Of the Cell, 12:685-698, 2001.

Pauletti, G.M., Gangwar, S., Okumu, F., et. al. Esterase-sensitive cyclic prodrugs of peptides: evaluation of an acyloxyalkoxy promoiety in a model hexapeptide. Pharm. Res., 13(11):1615-1623, 1996.

Perry, Chava, Sklan, Ella H., et. al. Complex Regulation of Acetylcholinesterase gene expression in human brain tumors. Oncogene, 21:8428-8441, 2002.

Pinto, M., Robine-Leon, S., Appay, M., et. al. Enterocyte-like differentiation and polarization of the human colon carcinoma cell line Caco-2 in culture. Biol. Cell, 47:323-330, 1983.

Plageman, L.R., Pauletti, G.M., Skau, K.A. Characterization of acetylcholinesterase in Caco-2 cells. Exp. Biol. Med., 227:480-486, 2002.

Sapin C., Colord, O., Delmas, O., et. al. Rafts promote assembly and apical targeting of a non-enveloped virus, rotavirus, in Caco-2 cells. J. Virol., 76(9):4591-45602, 2002.

Schroeder, Roxann J., Sharmin, Ahmed N., et. al. Cholesterol and sphingolipid enhance the Triton X- 100 insolubility of glycosylphosphatidylinositol-anchored proteins by promoting the formation of detergent-insoluble ordered membrane domains. J. Biol. Chem., 273(2):1150-1157, 1998.

Sharma, K. and Bigbee, J. Acetylcholinesterase antibody treatment results in neurite detachment and reduced outgrowth from cultured neurons: further evidence for a cell adhesive role for neuronal acetylcholinesterase. J. Neurosci. Res., 53:454-464, 1998.

Sheets, E. D., Holowka, D., and Baird, B. Membrane organization in immunoglobulin E receptor signaling. Curr. Opin. Chem. Biol., 3:95-99, 1999.

Simons, Kai and Ilkonen, Elina. Functional rafts in cell membranes. Nature 387:569-572, 1997.

Simons, Kai and Toomre, Derek. Lipid Rafts and Signal Transduction. Nature Reviews, 1:31-41, 2000.

Simons, Mikael, Friedrichson T., et. al. Exogenous administration of gangliosides displaces GPI-anchored proteins from lipid microdomains in living cells. Mol. Biol. of the Cell, 10:3187-3196, 1999.

Sine, J., Ferrand, R., Cloarec, P., et. al. Human intestine epithelial cell acetyl- and butyrylcholinesterase. Mol. and Cell. Biochemistry, 108:145-149, 1991.

Soreq, Hermona and Seidman, Shlomo. Acetylcholinesterase-new roles for an old actor. Nature, 2:294-302, 2001.

Soreq, H., Zakut, H. Human Cholinesterases and Anticholinesterases. Harcourt Brace and Company, San Diego, CA, 1993.

Stauffer, T.P., and Meyer, T. Compartmentalized IgE receptor-mediated signal transduction in living cells. J. Cell Biol., 139:1447-1454, 1997.

Sussman, J. L. et al. Atomic structure of acetylchlinesterase from *Torpedo californica*: a prototypic acetylcholine-binding protein. Science, 253:872-879, 1991.

Valero, Javier Saez and Vidal, Cecilio J. Monomers and dimers of acetylcholinesterase in human meningioma are anchored to the membrane by glycophosphatidylinositol. Neuroscience Letters, 195:101-104, 1995.

van't Hof, W., and van Meer, G. Generation of lipid polarity in intestinal epithelial (Caco-2) cells: sphingolipid synthesis in the Golgi complex and sorting behavior before vesicular traffic to the plasma membrane. J. Cell Biol., 111:977-986, 1990.

Wanner, A., Salathe, M, O'Riordan, T. G. Mucociliary clearance in the airways. Am. J. Respir. Crit. Care Med. 154:1868-1902, 1996.

Wang, Y., et. al. Human bronchial epithelial and endothelieal cells express α7 nicotinic acetylcholine receptors. Mol. Pharmacology, 60(6):1201-1209, 2001.

Zajchowski, Laura D., and Robbins, Stephen M. Lipid Rafts and Little Caves: compartmentalized signaling in membrane microdomains. Eur. J. Biochem., 269:737-752, 2002.